

UNIVERSITY OF UTRECHT

BACHELOR THESIS

**The bifurcation diagram of the second
nontrivial normal form of an axially
symmetric perturbation of the isotropic
harmonic oscillator**

Author:
T. Welker

Supervisor:
Dr. H. Hanßmann

August 26, 2014

Contents

1	Introduction	2
2	The Hamiltonian	5
2.1	The phase space	5
2.2	The first nontrivial normal form	6
2.3	The second nontrivial normal form	7
2.4	Nodal-Lissajous variables	9
3	Equilibria	11
4	The singular point $\tau = (0, 1, 0)$	13
4.1	The bifurcation lines concerning $\tau = (0, 1, 0)$	13
4.2	The intersection with $\mu = \pm 1$	15
4.3	The intersection with $\mu = 0$	16
4.4	The stability of $\tau = (0, 1, 0)$	18
5	The singular point $\tau = (0, 0, 0)$	23
5.1	The bifurcation lines concerning $\tau = (0, 0, 0)$	23
5.2	The stability of $\tau = (0, 0, 0)$	25
6	The equilibria at regular points	28
6.1	Regular equilibria on the upper arc of the phase space	32
6.2	Regular equilibria on the lower arc of the phase space	35
7	The bifurcation diagram	36
8	Global bifurcations	41
9	Conclusion	45

1 Introduction

In this thesis we study the dynamics of an axially symmetric perturbation of the isotropic harmonic oscillator. This dynamical system with three degrees of freedom serves as a model in many fields of science. For instance in astrophysics the motions of triaxial and axially symmetric galaxies can be described by a Hamiltonian system in 1-1-1 resonance. Thus, the analysis of the dynamics of the latter is essential for the understanding of the behaviour of triaxial and axially symmetric galaxies [12]. Also in molecular dynamics perturbations of harmonic oscillators are used to describe the motion of the nuclei in small molecules [3].

The Hamiltonian function H_ϵ we treat in this thesis can be described by

$$H_\epsilon(x, p) = \frac{1}{2}(p|p) + \frac{1}{2}\omega^2(x|x) + \epsilon(\frac{1}{3}\alpha x_3^3 + \beta(x_1^2 + x_2^2)x_3), \quad (1)$$

where $(\cdot|\cdot)$ denotes the standard inner product. The small parameter ϵ is introduced by a scaling $x \mapsto \epsilon x$, $p \mapsto \epsilon p$, $H \mapsto \epsilon^2 H$, hence H_ϵ describes the dynamics close to the origin. In this thesis we put the frequency ω to 1 by scaling time. Parameters α and β are external parameters, the perturbing force field depends upon. By a scaling

$$\alpha \mapsto \frac{\alpha}{\|(\alpha, \beta)\|}, \quad \beta \mapsto \frac{\beta}{\|(\alpha, \beta)\|}, \quad \epsilon \mapsto \epsilon \|(\alpha, \beta)\|$$

we make α and β of order 1, e.g. $\alpha^2 + \beta^2 = 1$. If by doing this ϵ gets too big, we can once again rescale all variables so that again H_ϵ describes the dynamics close to the origin. We mention two other parameters: the third component of the angular momentum $N = x_1 p_1 - x_2 p_2$ and the energy L of the unperturbed Hamiltonian, i.e. $H_0 = L$. Note that since H_ϵ is axially symmetric, N is an integral of motion by Noether's theorem. For the same reason L is an integral of motion for H_0 .

The main source of information for this thesis is [4]. In this paper the same Hamiltonian system is treated, focusing on the dynamics of the first nontrivial normal form \bar{H}_ϵ . By carrying out a normalization process and truncating the higher order terms, the first nontrivial normal form \bar{H}_ϵ (or, as they put it, the normal form of order 2) has got N and L as integrals of motion. Thus, we can fix the value a of N and the value b of L . The periodic flows of N

and L can be used to reduce our system to a one degree of freedom system. In [4] the regions of external parameters α and β are studied where the one degree of freedom system defined by \bar{H}_ϵ (and parameterized by a and b) is structurally stable. It turns out that there are six interesting cases. At $\beta = 0$, $6\alpha = \beta$, $\alpha = 2\beta$ and $\alpha = 5\beta$ the family (1) is structurally stable. At $\alpha = 2\beta$ and $\alpha = 5\beta$ a Hamiltonian Hopf bifurcation occurs for the first nontrivial normal form, see [7, 8]. The case $\beta = 0$ corresponds to a parameter value where H_ϵ is integrable, see [9]. The system is also integrable at $\alpha = 6\beta$, but here the normal form is structurally stable and no bifurcation occurs. At $\alpha = \beta$ the family (1) is not structurally stable and H_ϵ is again integrable. It is shown in [7] that this integrability leads to a degeneracy of the normal form through all orders. At $\alpha = -\beta$ the first nontrivial normal form is also not structurally stable. At this parameter value H_ϵ is the system originally studied by Hénon and Heiles. A higher order normal form is needed to correctly resolve the \mathbb{Z}_3 -equivariant dynamics. Hence our main goal in this thesis is to study the dynamics of the second nontrivial normal form, as is calculated in [7] and [8], with the region around $\alpha = -\beta$ of our main concern.

This thesis is organized as follows. Chapter 2 discusses the basic aspects developed and found in [4], [7] and [11]. We describe the reduced phase space of the Hamiltonian system and see that it has, depending on the parameters of our system, one or two singularities. We also give the second nontrivial normal form as calculated in [7] and introduce the set of nodal-Lissajous variables. In chapter 3 we explore the conditions for the equilibria of the Hamiltonian system. We will see that the singular point(s) of the phase space are always equilibria. Furthermore we find one equation that can be solved for the regular equilibria, depending on the parameters of our system. In chapter 4 we investigate the stability of the singular point of the phase space that is always present. To do this, we introduce the notion of (Lyapunov) stability. We will see that flip bifurcations occur. In chapter 5 we look at the stability of the other singular point, whenever it exists. We will see that Hamiltonian Hopf bifurcations occur. In chapter 6 we study the equilibria at regular points. We will detect that centre-saddle bifurcations take place. We will see that we need to use the nodal-Lissajous variables to obtain an analytic expression of this bifurcation line. In chapter 7 we give the bifurcation diagram of the second nontrivial normal form. In this section we also give pictures showing the flow of the Hamiltonian on the phase space for each area in the bifurcation diagram. The bifurcation diagram suggests

that global bifurcations may occur. In chapter 8 we attempt to calculate when these global bifurcations occur.

2 The Hamiltonian

In this first chapter we will give an overview of the main results already established when studying (1), so that we have machinery to work with for what will come in this thesis.

2.1 The phase space

Naturally the Hamiltonian (1) is defined on a six-dimensional phase space $\mathbb{R}^3 \times \mathbb{R}^3$. Since H_ϵ has N as an integral of motion we can, by fixing the value a of N , perform a reduction to a two-degree-of-freedom system. By normalising H_ϵ the symmetry of H_0 is pushed through the Taylor series of the Hamiltonian and truncation yields a normal form of the Hamiltonian with an extra symmetry. In this way we obtain another integral of motion: L . We can use this to reduce to a one degree of freedom system. This results in a phase space $V_{a,b} \subseteq \mathbb{R}^3$ such that $\dim(V_{a,b})=2$. It turns out (see[4]) that

$$V_{a,b} = \{\tau \in \mathbb{R}^3 \mid R_{a,b}(\tau) = 0, 2|a| \leq \tau_2 \leq 2b\}$$

where

$$R_{a,b}(\tau) = \tau_1^2 + \tau_3^2 - (\tau_2 - 2b)^2(\tau_2^2 - 4a^2).$$

To further simplify we rescale

$$\tau_1 \mapsto 4b^2\tau_1, \tau_2 \mapsto 2b\tau_2 \text{ and } \tau_3 \mapsto 4b^2\tau_3 \quad (2)$$

such that the phase space becomes

$$V_\mu = \{\tau \in \mathbb{R} \times [|\mu|, 1] \times \mathbb{R} \mid R_\mu(\tau) = 0\}. \quad (3)$$

Here $\mu = \frac{a}{b} \in [-1, 1]$ and

$$R_\mu(\tau) = \tau_1^2 + \tau_3^2 - (\tau_2 - 1)^2(\tau_2^2 - \mu^2).$$

The phase space is a surface of revolution around the τ_2 -axis, see figure 1. For $\mu = 0$ the space has two singularities, $\tau = (0, 0, 0)$ and $\tau = (0, 1, 0)$, and is lemon-shaped. For $\mu \neq 0$ the space has only one singularity, $\tau = (0, 1, 0)$, and is turnip-shaped. For convenience we will sometimes call $\tau = (0, 0, 0)$ point P and $\tau = (0, 1, 0)$ point Q. Note that for $\mu = \pm 1$ the phase space consists of the single point $\tau = (0, 1, 0)$.

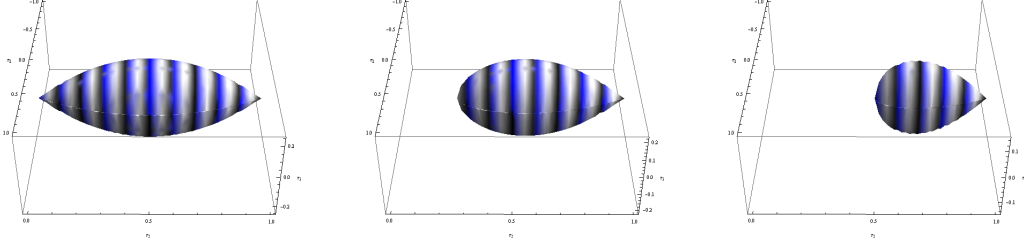


Figure 1: The phase space for $\mu = 0$, $\mu = 0.25$ and $\mu = 0.5$.

2.2 The first nontrivial normal form

Normalization is an iterative process using a coordinate transformation on H_ϵ such that the Hamiltonian is simplified. Every step in this iterative process can add extra terms to the normal form. In this case all normal form terms of odd degree vanish. The first nontrivial normal form is obtained by normalizing two times and is of degree four in (x, p) . After using that N and L are integrals of motion to reduce the degrees of freedom, we obtain the first nontrivial normal form

$$\begin{aligned} \tilde{H}_\epsilon^{a,b;\lambda}(\tau) = & b + \frac{\epsilon^2}{48}(-20b^2 - 4a^2\lambda^2 + 2\lambda(1 - 6\lambda)\tau_1 \\ & + 4b(5 - 6\lambda - 4\lambda^2)\tau_2 - (5 - 12\lambda - 3\lambda^2)\tau_2^2), \end{aligned} \quad (4)$$

where $\lambda = \beta/\alpha$, on the phase space $V_{a,b}$, see [4] for details on the calculation. To simplify we divide $\tilde{H}_\epsilon^{a,b;\lambda}$ by $(\epsilon^2/48)$, omit the constant terms and rescale time, obtaining

$$\bar{H}^{a,b;\lambda}(\tau) = 2\lambda(1 - 6\lambda)\tau_1 + 4b(5 - 6\lambda - 4\lambda^2)\tau_2 - (5 - 12\lambda - 3\lambda^2)\tau_2^2, \quad (5)$$

again defined on the phase space $V_{a,b}$. To further simplify we scale τ according to (2), divide $\bar{H}^{a,b;\lambda}$ by $4b^2$ and rescale time again. This gives the Hamiltonian function

$$H^\lambda(\tau) = 2\lambda(1 - 6\lambda)\tau_1 + 2(5 - 6\lambda - 4\lambda^2)\tau_2 - (5 - 12\lambda - 3\lambda^2)\tau_2^2 \quad (6)$$

defined on the phase space V_μ . Of course we could have gone from (4) directly to (6) by rescaling τ , dividing $\tilde{H}_\epsilon^{a,b;\lambda}$ by $(\epsilon^2 b^2/12)$ and scaling the time, but we will use the simplest Hamiltonian function with τ not scaled in section 6.

Notice that the dependence of H^λ on λ and the dependence of V_μ on μ makes the Hamiltonian system depending on only two parameters, with $\lambda \in \mathbb{R}$ and $\mu \in [-1, 1]$. Also notice that H^λ is independent of τ_3 .

2.3 The second nontrivial normal form

The second nontrivial normal form, as calculated in [7] and [8], is obtained by normalizing four times and is of degree six in (x, p) . After reducing it by using that N and L are integrals of motion, the second nontrivial normal form can be written as

$$\tilde{\mathcal{H}}_\epsilon^{a,b;\lambda}(\tau) = \tilde{H}_\epsilon^{a,b;\lambda}(\tau) + \frac{\epsilon^4}{3456} \tilde{K}_\epsilon^{a,b;\lambda}(\tau),$$

where $\tilde{H}_\epsilon^{a,b;\lambda}$ is defined in (4) and

$$\begin{aligned} \tilde{K}_\epsilon^{a,b;\lambda}(\tau) = & -8a^2\lambda^2(43 - 372\lambda + 369\lambda^2) + 4b\lambda(41 - 42\lambda - 656\lambda^2 - 48\lambda^3)\tau_1 \\ & - 2\lambda(1 - \lambda)(41 - 61\lambda - 606\lambda^2)\tau_2\tau_1 \\ & + 4b^2(705 - 720\lambda - 251\lambda^2 - 972\lambda^3 - 172\lambda^4)\tau_2 \\ & - 4a^2(43 - 372\lambda + 369\lambda^2)\tau_2 \\ & - 2b(705 - 1440\lambda + 189\lambda^2 - 1764\lambda^3 + 900\lambda^4)\tau_2^2 \\ & + 5(1 - \lambda)(47 - 97\lambda - 9\lambda^2 - 201\lambda^3)\tau_2^3, \end{aligned}$$

defined on the phase space $V_{a,b}$. Again we simplify by dividing $\tilde{\mathcal{H}}_\epsilon^{a,b;\lambda}$ by $(\epsilon^2/48)$, omitting the constant terms and rescaling time. By doing this we obtain

$$\bar{\mathcal{H}}_\epsilon^{a,b;\lambda}(\tau) = \bar{H}_\epsilon^{a,b;\lambda}(\tau) + \frac{\epsilon^2}{72} \bar{K}_\epsilon^{a,b;\lambda}(\tau),$$

where $\bar{H}_\epsilon^{a,b;\lambda}$ is defined in (5) and

$$\begin{aligned} \bar{K}_\epsilon^{a,b;\lambda}(\tau) = & 4b\lambda(41 - 42\lambda - 656\lambda^2 - 48\lambda^3)\tau_1 \\ & - 2\lambda(1 - \lambda)(41 - 61\lambda - 606\lambda^2)\tau_2\tau_1 \\ & + 4b^2(705 - 720\lambda - 251\lambda^2 - 972\lambda^3 - 172\lambda^4)\tau_2 \\ & - 4a^2(43 - 372\lambda + 369\lambda^2)\tau_2 \\ & - 2b(705 - 1440\lambda + 189\lambda^2 - 1764\lambda^3 + 900\lambda^4)\tau_2^2 \\ & + 5(1 - \lambda)(47 - 97\lambda - 9\lambda^2 - 201\lambda^3)\tau_2^3. \end{aligned}$$

After rescaling τ according to (2), dividing $\bar{\mathcal{H}}_\epsilon^{a,b;\lambda}$ by $4b^2$ and rescaling time, the second nontrivial normal form on the phase space V_μ can be written as

$$\mathcal{H}_\delta^{\lambda,\mu}(\tau) = H^\lambda(\tau) + \delta K_\mu^\lambda(\tau), \quad (7)$$

where $\delta = \epsilon^2 b/36$, $H^\lambda(\tau)$ is defined in (6), and

$$\begin{aligned}
K_\mu^\lambda(\tau) = & 2\lambda(41 - 42\lambda - 656\lambda^2 - 48\lambda^3)\tau_1 \\
& - 2\lambda(1 - \lambda)(41 - 61\lambda - 606\lambda^2)\tau_2\tau_1 \\
& + (705 - 720\lambda - 251\lambda^2 - 972\lambda^3 - 172\lambda^4)\tau_2 \\
& - \lambda^2(43 - 372\lambda + 369\lambda^2)\mu^2\tau_2 \\
& - (705 - 1440\lambda + 189\lambda^2 - 1764\lambda^3 + 900\lambda^4)\tau_2^2 \\
& + 5(1 - \lambda)(47 - 97\lambda - 9\lambda^2 - 201\lambda^3)\tau_2^3.
\end{aligned}$$

Notice that the second nontrivial normal form does depend on the parameter μ and that there are terms depending on both τ_1 and τ_2 , but $\mathcal{H}_\delta^{\lambda,\mu}$ is still independent of τ_3 .

The behaviour of the second nontrivial normal form should be determined mainly by $H^\lambda(\tau)$. For small λ this is indeed the case, since δ is small. But for very large values of λ the behaviour of $K_\mu^\lambda(\tau)$ will dominate since it is of higher degree in λ . This problem can be overcome by not introducing the quotient of α and β . We first write the normal form in terms of α and β rather than λ . Since $H^\lambda(\tau)$ is of degree 2 in λ , we multiply the whole equation with α^2 and substitute (since $\lambda = \frac{\beta}{\alpha}$)

$$\alpha^2 \rightarrow \alpha^2, \lambda\alpha^2 \rightarrow \beta\alpha, \lambda^2\alpha^2 \rightarrow \beta^2.$$

$K_\mu^\lambda(\tau)$ is of degree 4 in λ , so we multiply the whole equation with α^4 and substitute

$$\alpha^4 \rightarrow \alpha^4, \lambda\alpha^4 \rightarrow \beta\alpha^3, \lambda^2\alpha^4 \rightarrow \beta^2\alpha^2, \lambda^3\alpha^4 \rightarrow \beta^3\alpha, \lambda^4\alpha^4 \rightarrow \beta^4.$$

We have now obtained the second nontrivial normal form written in α and β . Since $\alpha^2 + \beta^2 = 1$ we can put $\alpha = \cos \phi$ and $\beta = \sin \phi$ and consider $\phi \in [0, \pi]$, as done in [10]. In this way the normal form depends on bounded functions of the parameter ϕ , hence for all $\phi \in [0, \pi]$ the first nontrivial normal form will be mainly determining the behaviour of the Hamiltonian. Explicitly we write the second nontrivial normal form as

$$\mathcal{H}_\mu^{\alpha,\beta,\delta}(\tau) = a_1\tau_1 + a_2\tau_2\tau_1 + (b_1 + \mu^2b_2)\tau_2 + c\tau_2^2 + d\tau_2^3 \quad (8)$$

with $\tau \in \mathbb{R} \times [|\mu|, 1] \times \mathbb{R}$ and

$$\begin{aligned}
a_1(\phi) &= 2(\cos \phi - 6 \sin \phi) \sin \phi \\
&\quad + \frac{\delta}{2}(-533 \cos \phi + 697 \cos 3\phi - 186 \sin \phi + 6 \sin 3\phi) \sin \phi \\
a_2(\phi) &= \delta(211 \cos \phi - 293 \cos 3\phi - 858 \sin \phi + 354 \sin 3\phi) \sin \phi \\
b_1(\phi) &= 1 + 9 \cos 2\phi - 6 \sin 2\phi \\
&\quad + \frac{\delta}{2}(337 + 877 \cos 2\phi + 196 \cos 4\phi - 846 \sin 2\phi + 63 \sin 4\phi) \quad (9) \\
b_2(\phi) &= \delta(-206 + 163 \cos 2\phi + 186 \sin 2\phi) \sin^2 \phi \\
c(\phi) &= -1 - 4 \cos 2\phi + 6 \sin 2\phi \\
&\quad - \frac{3\delta}{2}(417 - 65 \cos 2\phi + 118 \cos 4\phi - 534 \sin 2\phi + 27 \sin 4\phi) \\
d(\phi) &= 5\delta(104 - 77 \cos 2\phi + 20 \cos 4\phi - 84 \sin 2\phi + 6 \sin 4\phi).
\end{aligned}$$

Notice that (7) can also be written in the form (8) but with coefficients a_1 , a_2 , b_1 , b_2 , c and d depending on λ . So from now onwards we will drop the dependence of the coefficients on ϕ or λ and only choose one over the other if we explicitly want to give a formula in ϕ or λ . Note that we can go from one to the other by writing $\lambda = \tan \phi$. We also see that both the phase space and the equation of the Hamiltonian are invariant under the reflection $\mu \mapsto -\mu$, so our bifurcation diagram will be invariant under this reflection as well.

2.4 Nodal-Lissajous variables

When describing the dynamics of our Hamiltonian system, different sets of variables will be used. We started with the expression of our Hamiltonian function H_ϵ in the classical variables $(x_1, x_2, x_3, p_1, p_2, p_3) \in \mathbb{R}^6$. When we introduced the first and second nontrivial normal form we switched to the use of $(\tau_1, \tau_2, \tau_3) \in \mathbb{R} \times [|\mu|, 1] \times \mathbb{R}$. This gave an efficient way to define the phase space and the normal forms. But we will see that there is another set of variables that we need to consider: the nodal-Lissajous variables.

The set (l, g, v, L, G, N) is called the nodal-Lissajous variables and is obtained by performing two canonical transformations on $(x_1, x_2, x_3, p_1, p_2, p_3)$. Recall that L is the energy of the unperturbed Hamiltonian and N the third component of the angular momentum. Furthermore, G is the total angular momentum: $G = \|\vec{x} \times \vec{p}\|$. The conjugate angle variables are l , g and v . While N and L are fixed after normalization, G still varies. For a complete

introduction of the nodal-Lissajous variables we refer to [4, 11]. For completeness we state the domains of the nodal-Lissajous variables: $l, g, v \in [0, 2\pi)$, $L > 0$, $0 < G < L$ and $|N| < G$.

The relation between the nodal-Lissajous variables and the unscaled τ , as calculated in [4, 11], is

$$\begin{aligned}
\tau_1 &= 2 \left(1 - \frac{a^2}{G^2}\right) (b^2 - G^2 + b\sqrt{b^2 - G^2} \cos 2g) \\
&\quad - \left(1 - \frac{a^2}{G^2}\right)^2 (b + \sqrt{b^2 - G^2} \cos 2g)^2 \\
\tau_2 &= b - \sqrt{b^2 - G^2} \cos 2g + \frac{a^2}{G^2} (b + \sqrt{b^2 - G^2} \cos 2g) \\
\tau_3 &= 2 \left(1 - \frac{a^2}{G^2}\right) G \sqrt{b^2 - G^2} \sin 2g.
\end{aligned} \tag{10}$$

3 Equilibria

The equilibria of the Hamiltonian system are those places where the level set of the Hamiltonian $\{\tau \in \mathbb{R}^3 \mid \mathcal{H}_\mu^{\alpha,\beta,\delta}(\tau) = h\}$ is tangent to the phase space $V_\mu \subseteq \mathbb{R}^3$. Note that the singular point(s) of the phase space are always equilibria. Since $\mathcal{H}_\mu^{\alpha,\beta,\delta}$ is independent of τ_3 , its level set, and therefore its tangent space, will always contain the whole τ_3 -axis. So for an equilibrium, the tangent space of the phase space should also include the whole τ_3 -axis. As explained in section 2.1, the phase space is a surface that is invariant under rotation around the τ_2 -axis. Hence a tangent plane is only containing the τ_3 -axis if the τ_3 -coordinate of that point is zero. To summarize, all equilibria are found on the section $V_\mu \cap \{\tau_3 = 0\}$ of the phase space.

We further investigate the conditions for the equilibria. As explained before, all singularities of the phase space are always equilibria, so we exclude the cases $\tau_2 = 0$ and $\tau_2 = 1$. The section $V_\mu \cap \{\tau_3 = 0\}$ is described by

$$\tau_1 = \pm(1 - \tau_2)\sqrt{\tau_2^2 - \mu^2}, \quad (11)$$

see (3), where the equation with the plus sign gives the upper arc of the projection of the phase space on $\tau_3 = 0$, and the equation with the minus sign gives the lower arc of this projection. The section $\{\mathcal{H}_\mu^{\alpha,\beta,\delta} = h\} \cap \{\tau_3 = 0\}$ is described by

$$\tau_1 = \frac{h - (b_1 + \mu^2 b_2)\tau_2 - c\tau_2^2 - d\tau_2^3}{a_1 + a_2\tau_2}, \quad (12)$$

see (8). First of all, since the level set of the Hamiltonian has to touch the phase space, the right hand sides of these two equations have to be equal. Hence we can express h in τ_2 and λ

$$h = (b_1 + \mu^2 b_2)\tau_2 + c\tau_2^2 + d\tau_2^3 \pm (a_1 + a_2\tau_2)(1 - \tau_2)\sqrt{\tau_2^2 - \mu^2}. \quad (13)$$

Second of all, the derivative of the right hand sides of (11) and (12) with respect to τ_2 have to be equal, so that the level set of the Hamiltonian is tangent to the phase space. The derivative of the right hand side of (11) is

$$\begin{aligned} \frac{\partial}{\partial \tau_2} \left(\pm(1 - \tau_2)\sqrt{\tau_2^2 - \mu^2} \right) &= \mp\sqrt{\tau_2^2 - \mu^2} \pm \frac{\tau_2(1 - \tau_2)}{\sqrt{\tau_2^2 - \mu^2}} \\ &= \pm \frac{(-\tau_2^2 + \mu^2 + \tau_2(1 - \tau_2))}{\sqrt{\tau_2^2 - \mu^2}}, \end{aligned}$$

resulting in the slope of the phase space

$$\pm \frac{(\mu^2 + \tau_2 - 2\tau_2^2)}{\sqrt{\tau_2^2 - \mu^2}}. \quad (14)$$

The derivative of the right hand side of (12) is

$$\begin{aligned} & \frac{\partial}{\partial \tau_2} \left(\frac{h - (b_1 + \mu^2 b_2) - c\tau_2^2 - d\tau_2^3}{a_1 + a_2\tau_2} \right) \\ &= \frac{-b_1 - \mu^2 b_2 - 2c\tau_2 - 3d\tau_2^2}{(a_1 + a_2\tau_2)} + \frac{a_2(-h + (b_1 + \mu^2 b_2)\tau_2 + c\tau_2^2 + d\tau_2^3)}{(a_1 + a_2\tau_2)^2}. \end{aligned} \quad (15)$$

Filling in the above found expression (13) for h gives the slope of the level set of the Hamiltonian function

$$\frac{-(b_1 + \mu^2 b_2) - 2c\tau_2 - 3d\tau_2^2}{a_1 + a_2\tau_2} \mp \frac{a_2(1 - \tau_2)\sqrt{\tau_2^2 - \mu^2}}{a_1 + a_2\tau_2}, \quad (16)$$

at points τ_2 with $(\tau_1, \tau_2, 0) \in V_\mu$. These two slopes have to be equal at a point of equilibrium, resulting in the following

$$\begin{aligned} & \pm (a_1 + a_2\tau_2)(\mu^2 + \tau_2 - 2\tau_2^2) \\ &= -\sqrt{\tau_2^2 - \mu^2}(b_1 + \mu^2 b_2 + 2c\tau_2 + 3d\tau_2^2) \mp a_2(1 - \tau_2)(\tau_2^2 - \mu^2), \end{aligned}$$

with the two plus-minus signs being related. This can be simplified to

$$\begin{aligned} & \pm(\mu^2(a_1 - a_2) + (a_1 + 2\mu^2 a_2)\tau_2 - 2(a_1 - a_2)\tau_2^2 - 3a_2\tau_2^3) \\ &= -\sqrt{\tau_2^2 - \mu^2}(b_1 + \mu^2 b_2 + 2c\tau_2 + 3d\tau_2^2). \end{aligned} \quad (17)$$

We have now found one equation that, depending on choice of μ and λ (or μ and ϕ), can be numerically solved for $\tau_2 \in [|\mu|, 1]$. One could even try to analytically solve this equation for τ_2 expressed in μ and λ since (17) can be rewritten as a polynomial function of degree six in τ_2 and solutions are the roots of this polynomial. This is however beyond the scope of this thesis. We actually obtained two equations; solving the one with a plus sign gives the equilibria on the upper arc of the phase space and solving the one with a minus sign gives the equilibria on the lower arc. Recall that the singularities of the phase space are always equilibria.

4 The singular point $\tau = (0, 1, 0)$

The stability of $\tau = (0, 1, 0)$, which we will also call point Q, solely depends on the way the level set of the Hamiltonian passes through $\tau = (0, 1, 0)$. There are three different cases to distinguish:

1. The level set of the Hamiltonian passes outside the phase space, hence the modulus of its slope at Q is larger than the modulus of the slope of the phase space at Q.
2. The level set of the Hamiltonian passes inside the phase space, hence the modulus of its slope at Q is smaller than the modulus of the slope of the phase space at Q.
3. The slope of the level set of the Hamiltonian is equal to the slope of the phase space at Q.

Solving the last equation results in the bifurcation lines concerning point Q. It was shown in [4] for the first nontrivial normal form that some of these bifurcation lines are flip bifurcations (also called period-doubling bifurcations). This will also happen for the second nontrivial normal form, we will come back to this point in section 4.4. What happens is that a stable periodic orbit bifurcates, loses its stability, and a new periodic orbit emerges with twice the period of the original one.

4.1 The bifurcation lines concerning $\tau = (0, 1, 0)$

We want to obtain an expression of the bifurcation lines concerning $\tau = (0, 1, 0)$ in ϕ and μ . We should work with ϕ rather than λ since $\tau = (0, 1, 0)$ also bifurcates for large values of λ (as we will see).

At Q the phase space can be approximated by the cone

$$\tau_1 = \pm(1 - \tau_2)\sqrt{1 - \mu^2}.$$

Filling in $\tau = (0, 1, 0)$ in (16) gives the slope of the level set of the Hamiltonian at Q

$$\frac{-(b_1 + \mu^2 b_2 + 2c + 3d)}{a_1 + a_2}.$$

So we want to solve

$$\frac{-(b_1 + \mu^2 b_2 + 2c + 3d)}{a_1 + a_2} = \mp \sqrt{1 - \mu^2}$$

for μ in terms of ϕ . Substituting $x = \sqrt{1 - \mu^2}$ the equation becomes

$$-(b_1 + (1 - x^2)b_2 + 2c + 3d) = \mp(a_1 + a_2)x.$$

Rearranging this gives a quadratic polynomial

$$b_2 x^2 \pm (a_1 + a_2)x - (b_1 + b_2 + 2c + 3d) = 0.$$

We have to distinguish two cases: $b_2 = 0$ and $b_2 \neq 0$. Suppose first that $b_2 = 0$. Thus, recalling the definition of b_2 ,

$$b_2(\phi) = \delta(-206 + 163 \cos 2\phi + 186 \sin 2\phi) \sin^2 \phi,$$

we have $\phi = 0$ or π , hence $a_1 = a_2 = 0$ and $b_1 + 2c + 3d = 0$, or $-206 + 163 \cos 2\phi + 186 \sin 2\phi = 0$, which doesn't give any solutions with $x \in [0, 1]$. So we have found two bifurcation lines: $\phi = 0$ and $\phi = \pi$. Suppose now that $b_2 \neq 0$, then we can solve the equation above for x , giving

$$x = \pm \left[\frac{a_1 + a_2}{2b_2} \pm' \sqrt{\frac{b_1 + b_2 + 2c + 3d}{b_2} + \frac{(a_1 + a_2)^2}{4b_2^2}} \right]$$

where the two plus-minus signs are unrelated. Since $\mu = \pm\sqrt{1 - x^2}$ and $\mu \in \mathbb{R}$, we should have $|x| \leq 1$. Therefore the second plus-minus sign should be a minus. We have now found an expression for μ

$$\mu = \pm \sqrt{1 - \left(\frac{a_1 + a_2}{2b_2} - \sqrt{\frac{b_1 + b_2 + 2c + 3d}{b_2} + \frac{(a_1 + a_2)^2}{4b_2^2}} \right)^2}. \quad (18)$$

We actually got two equations; one for μ being positive, the other for μ being negative. If we now substitute for a_1 , a_2 , b_1 , b_2 , c and d their expressions in ϕ , see (9), we obtain the explicit formula $\mu = \mu(\phi)$ of the bifurcation lines coming from $\tau = (0, 1, 0)$. These lines are the flip bifurcation lines, as we will see in section 4.4. Recall that $\phi = 0$ and $\phi = \pi$ are also bifurcation lines. The resulting graph of the bifurcation lines can be seen in figure 2.

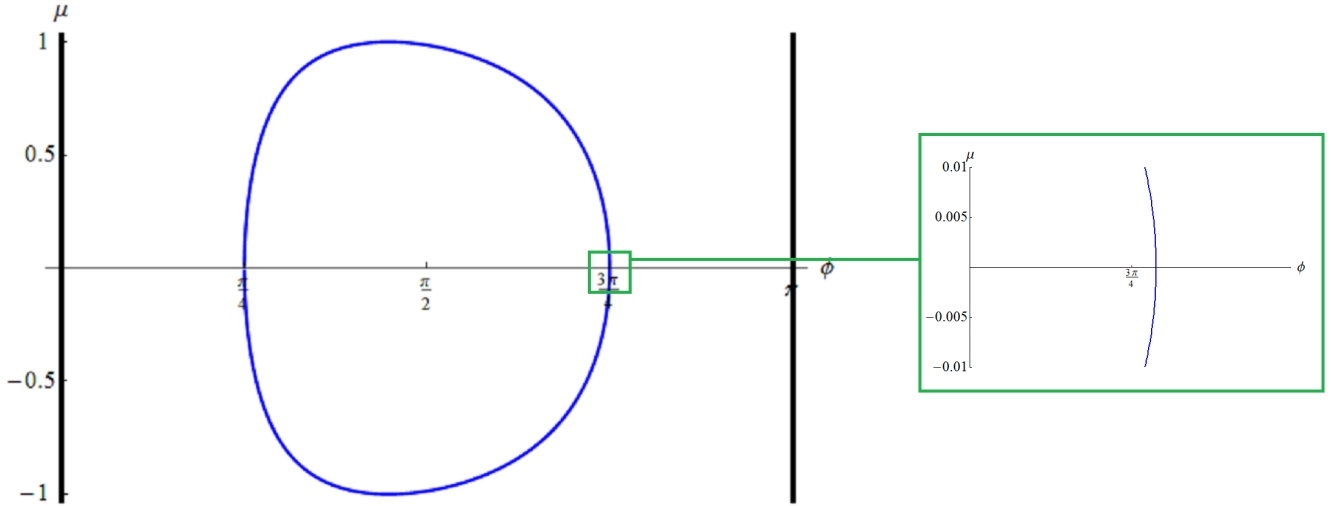


Figure 2: The bifurcation lines concerning $\tau = (0, 1, 0)$, portrayed for the case $\delta = 10^{-6}$. The magnification shows that the intersection of the bifurcation lines with the ϕ -axis does not happen at $\frac{3\pi}{4}$, but at a slightly larger value.

4.2 The intersection with $\mu = \pm 1$

As shown in [4] for the first nontrivial normal form, the bifurcation lines touch $\mu = \pm 1$ at $\lambda = 6$ (so at $\phi = \arctan(6)$). To see for which value(s) of ϕ this happens for the second nontrivial normal form, we use (18) and solve

$$\frac{a_1 + a_2}{2b_2} = \sqrt{\frac{b_1 + b_2 + 2c + 3d}{b_2} + \frac{(a_1 + a_2)^2}{4b_2^2}}$$

for ϕ . This can be simplified to

$$b_1 + b_2 + 2c + 3d = 0 \quad \text{so} \quad b_1 = -b_2 - 2c - 3d.$$

In table 1 the numerical solutions of this equation, depending on δ , are given. We see that for increasing values of δ , the point of intersection moves to the right.

Theorem 1. *The value of ϕ for which the line of flip bifurcations intersects with $\mu = \pm 1$ increases when δ increases, in a small neighbourhood around $(\arctan(6), 0)$. When $\delta \downarrow 0$ this value goes to $\phi = \arctan(6)$.*

	$b_1 = -b_2 - 2c - 3d$
$\delta = 0$	$\phi \approx 1.405648 = \arctan(6)$
$\delta = 10^{-7}$	$\phi \approx 1.405653$
$\delta = 10^{-6}$	$\phi \approx 1.405703$
$\delta = 10^{-5}$	$\phi \approx 1.406200$

Table 1: The numerical values for which the line of flip bifurcations touches $\mu = \pm 1$.

Proof. We apply the implicit function theorem. We write

$$f(\phi, \delta) = b_1 + b_2 + 2c + 3d$$

where b_1 , b_2 , c and d can be expressed in ϕ and δ , see (9). Note that $f(\phi, \delta)$ is a C^1 function on \mathbb{R}^2 . We know that $f(\arctan(6), 0) = 0$. Also

$$\frac{\partial f}{\partial \phi} \Big|_{(\arctan(6), 0)} = -12.$$

Hence the implicit function theorem is applicable: there is a C^1 function $\phi = \phi(\delta)$ defined on an open interval around $\delta = 0$ such that $\phi(0) = \arctan(6)$ and

$$\frac{d\phi}{d\delta}(0) = -\frac{\frac{\partial f}{\partial \delta} \Big|_{(\arctan(6), 0)}}{\frac{\partial f}{\partial \phi} \Big|_{(\arctan(6), 0)}} = -\frac{662.673}{-12} > 0.$$

Since $\frac{d\phi}{d\delta}(0) > 0$, we see that increasing δ gives a larger value of ϕ in a small neighbourhood around $\phi = \arctan(6)$ and $\delta = 0$. Furthermore, since $\phi(0) = \arctan(6)$, we see that if $\delta \downarrow 0$, then ϕ goes to $\arctan(6)$. \square

4.3 The intersection with $\mu = 0$

We are also interested for which ϕ these bifurcation lines go through the ϕ -axis. For the first nontrivial normal form this happens at $\lambda = -1$ and $\lambda = 1$, so at $\phi = \frac{\pi}{4}$ and $\phi = \frac{3\pi}{4}$. To calculate these points for the second nontrivial normal form we solve the following equation

$$1 = \left(\frac{a_1 + a_2}{2b_2} - \sqrt{\frac{b_1 + b_2 + 2c + 3d}{b_2} + \frac{(a_1 + a_2)^2}{4b_2^2}} \right)^2,$$

coming from (18). This can be written as

$$\frac{a_1 + a_2}{2b_2} \mp 1 = \sqrt{\frac{b_1 + b_2 + 2c + 3d}{b_2} + \frac{(a_1 + a_2)^2}{4b_2^2}},$$

where the plus-minus sign comes from first having to take the square root on both sides. Squaring both sides of the equation and multiplying with $4b_2^2$ gives

$$((a_1 + a_2) \mp 2b_2)^2 = 4b_2(b_1 + b_2 + 2c + 3d) + (a_1 + a_2)^2.$$

Notice that the terms $(a_1 + a_2)^2$ and $4b_2^2$ can be cancelled, and we are left with

$$\mp b_2(a_1 + a_2) = b_2(b_1 + 2c + 3d).$$

Recall that during the calculation of (18) we assumed that $b_2 \neq 0$, so we can simplify this to

$$b_1 = -2c - 3d \mp (a_1 + a_2).$$

If we take $\phi = \frac{\pi}{4}$ then

$$a_1 = -5 - \frac{705}{2}\delta, \quad a_2 = 0, \quad b_1 = a_1, \quad c = -a_1, \quad d = 0,$$

so we find that $\phi = \frac{\pi}{4}$ is a solution of the equation (with a minus sign) above, regardless of the choice of δ . Both 0 and π are solutions of the equation (both with a plus or minus sign) above. There is another solution that does depend on δ , for values slightly larger than $\phi = \frac{3\pi}{4}$, of the equation with a plus sign. The ϕ -coordinate of this point in the parameter plane (ϕ, μ) will be called Y. The numerical values can be found in table 2.

Theorem 2. *Y increases when δ increases, in a small neighbourhood around $(\phi = \frac{3\pi}{4}, \delta = 0)$. Moreover, if $\delta \downarrow 0$ then this value goes to $\frac{3\pi}{4}$.*

Proof. Again we apply the implicit function theorem. We write

$$g(\phi, \delta) = b_1 + 2c + 3d - a_1 - a_2.$$

Note that $g(\phi, \delta)$ is a C^1 function on \mathbb{R}^2 . We know that $g(\frac{3\pi}{4}, 0) = 0$. Also

$$\frac{\partial g}{\partial \phi} \Big|_{(\frac{3\pi}{4}, 0)} = -10.0002.$$

	$b_1 = -2c - 3d + a_1 + a_2$
$\delta = 0$	$\phi \approx 2.356194 = \arctan(-1) = \frac{3\pi}{4}$
$\delta = 10^{-7}$	$\phi \approx 2.356202$
$\delta = 10^{-6}$	$\phi \approx 2.356270$
$\delta = 10^{-5}$	$\phi \approx 2.356949$

Table 2: The numerical values of Y : a flip bifurcation occurs with $(\phi, \mu) = (Y, 0)$.

Hence the implicit function theorem is applicable: there is a C^1 function $\phi = \phi(\delta)$ defined on an open interval around $\delta = 0$ such that $\phi(0) = \frac{3\pi}{4}$ and

$$\frac{d\phi}{d\delta}(0) = -\frac{\frac{\partial g}{\partial \delta}\big|_{(\frac{3\pi}{4}, 0)}}{\frac{\partial g}{\partial \phi}\big|_{(\frac{3\pi}{4}, 0)}}.$$

Computing this derivative gives that $\frac{d\phi}{d\delta}(0) = -\frac{756}{-10.0002} > 0$, so indeed we see that increasing δ gives a larger value of ϕ on a small neighbourhood around $(\frac{3\pi}{4}, 0)$. Also, if $\delta \downarrow 0$ then this value goes to $\frac{3\pi}{4}$. \square

4.4 The stability of $\tau = (0, 1, 0)$

Let $\Psi : \mathbb{R} \times V_\mu \mapsto V_\mu$ be the flow of the Hamiltonian $\mathcal{H}_\mu^{\alpha, \beta, \delta}$. Suppose p_e is a point of equilibrium of the flow.

Definition 1. We call p_e (Lyapunov) stable if $\forall \epsilon > 0 \exists \delta > 0$ such that

$$\|p(0) - p_e\| < \delta \Rightarrow \forall t \geq 0 \|p(t) - p_e\| < \epsilon \quad .$$

Suppose the level set of the Hamiltonian passes outside the phase space. Figure 3 shows the trajectories for different starting values $p(0)$. We see that if we move $p(0)$ closer to point Q , the whole trajectory is closer to Q . Hence for all $\epsilon > 0$ we can find a $\delta > 0$ such that if $\|p(0) - Q\| < \delta$ then $\|p(t) - Q\| < \epsilon$ for all $t \geq 0$. So point Q is stable.

Suppose the level set of the Hamiltonian passes inside the phase space. In figure 4 several trajectories can be seen. Suppose ϵ is chosen as indicated in figure 4. Then we can't find a $\delta > 0$ such that if $\|p(0) - Q\| < \delta$ then $\|p(t) - Q\| < \epsilon$, since for any choice of $p(0) \neq Q$, the maximal distance that

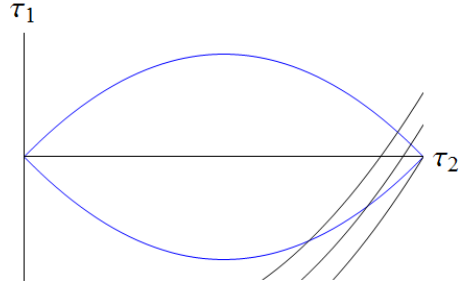


Figure 3: The level set of the Hamiltonian passes outside the phase space. The black lines denote the level set of the Hamiltonian for different values of $p(0)$. For simplicity we only show the projections of the phase space and of the level set of the Hamiltonian on $\{\tau_3 = 0\}$.

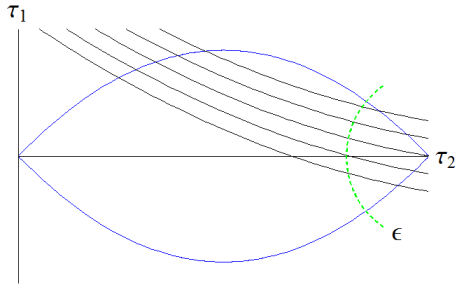


Figure 4: The level set of the Hamiltonian passes inside the phase space. The black lines denote the level set of the Hamiltonian for different $p(0)$. The radius of the dashed circle around point Q depicts a chosen value of ϵ .

$p(t)$ has to point Q is larger than ϵ . Hence point Q is not stable.

If the slope of the level set of the Hamiltonian is equal to the slope of the phase space at $\tau = (0, 1, 0)$, we should look at the second derivative to see if the Hamiltonian passes outside the phase space or not. First, for the phase

space, we take the derivative of (14) with respect to τ_2 , resulting in

$$\begin{aligned} & \frac{\partial}{\partial \tau_2} \left(\pm \frac{(\mu^2 + \tau_2 - 2\tau_2^2)}{\sqrt{\tau_2^2 - \mu^2}} \right) \\ &= \frac{\pm(1 - 4\tau_2)\sqrt{\tau_2^2 - \mu^2} \mp \tau_2(\mu^2 + \tau_2 - 2\tau_2^2)(\tau_2^2 - \mu^2)^{-1/2}}{\tau_2^2 - \mu^2} \\ &= \frac{\pm(-\mu^2 + 3\mu^2\tau_2 - 2\tau_2^3)}{(\tau_2^2 - \mu^2)^{3/2}}. \end{aligned}$$

We are interested in what happens at $\tau = (0, 1, 0)$, so we fill in $\tau_2 = 1$ to get the second derivative of the phase space at point Q

$$\mp \frac{2}{(1 - \mu^2)^{1/2}}. \quad (19)$$

Now we calculate the second derivative of the level set of the Hamiltonian. We first take the derivative of (15) with respect to τ_2 , giving

$$\begin{aligned} & \frac{\partial}{\partial \tau_2} \left(\frac{-b_1 - \mu^2 b_2 - 2c\tau_2 - 3d\tau_2^2}{(a_1 + a_2\tau_2)} + \frac{a_2(-h + (b_1 + \mu^2 b_2)\tau_2 + c\tau_2^2 + d\tau_2^3)}{(a_1 + a_2\tau_2)^2} \right) \\ &= \frac{-2a_1^2(c + 3d\tau_2) + 2a_1 a_2(b_1 + \mu^2 b_2 - 3d\tau_2^2) - 2a_2^2(-h + d\tau_2^3)}{(a_1 + a_2\tau_2)^3}. \end{aligned}$$

Filling in (13) for h gives

$$\frac{-2a_1(c + 3d\tau_2) + 2a_2(b_1 + \mu^2 b_2 + c\tau_2) \pm 2a_2^2(1 - \tau_2)\sqrt{\tau_2^2 - \mu^2}}{(a_1 + a_2\tau_2)^2},$$

the second derivative of the level set of the Hamiltonian function at points τ_2 with $(\tau_1, \tau_2, 0) \in V_\mu$. Again we fill in $\tau_2 = 1$ to obtain the value of the second derivative at point Q of the level set of the Hamiltonian

$$\frac{-2a_1(c + 3d) + 2a_2(b_1 + \mu^2 b_2 + c)}{(a_1 + a_2)^2}. \quad (20)$$

We want to compare the derivatives (19) and (20) at the flip bifurcations. We have found (18), an expression of μ in terms of ϕ for the flip bifurcations. We substitute this expression into (19) and (20) and then plot the resulting equations for $\phi \in [\frac{\pi}{4}, Y]$. From the resulting graph, see figure 5, we can conclude that at the bifurcation lines the Hamiltonian passes outside the phase

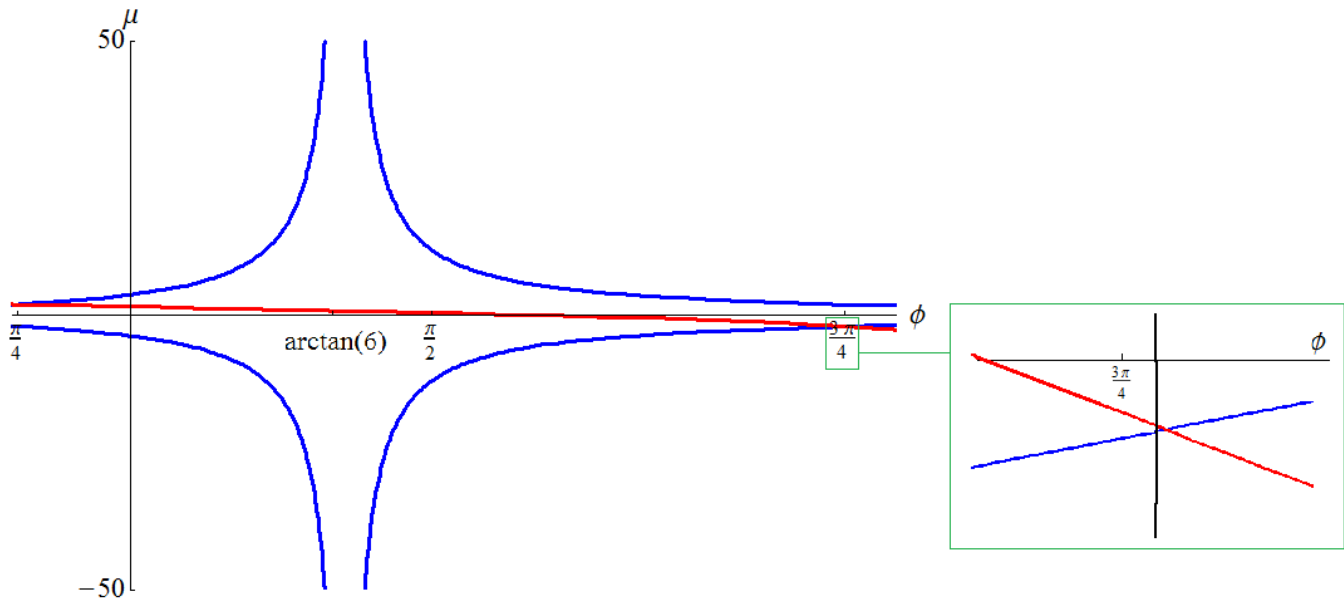


Figure 5: The blue lines are the values of the second derivative of the phase space at point Q, for the case that point Q bifurcates. The red line is the second derivative of the level set of the Hamiltonian at Q. We have zoomed in at the area around $\phi = \frac{3\pi}{4}$, to show that these lines cross after point Y we have also included the flip bifurcation line in black.

space, thus point Q is stable (see figure 6), except at $\phi = \frac{\pi}{4}$ and where the bifurcation lines touch $\mu = \pm 1$. Where the line of flip bifurcations touches $\mu = \pm 1$, the second derivative is obviously not continuous.

For the two points at which the bifurcation lines touch $\mu = \pm 1$, the single point of $V_{\pm 1}$ bifurcates. At $(\mu = 0, \phi = \frac{\pi}{4})$ the whole lower arc of the phase space consists of equilibria. That is, the level set of the Hamiltonian that passes through Q coincides with the lower arc, see figure 7. We see that all the equilibria on the lower arc are unstable: we can't find for all $\epsilon > 0$ a $\delta > 0$ such that if $\|p(0) - p_e\| < \delta$ then $\|p(t) - p_e\| < \epsilon$.

The bifurcation lines, apart from $(\mu = 0, \phi = \frac{\pi}{4})$ and where the single point of $V_{\pm 1}$ bifurcates, represent flip bifurcations. This is proven in [4] for the first nontrivial normal form (and is still valid for higher order normal forms). For

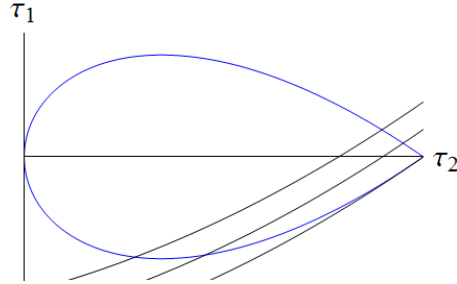


Figure 6: On the bifurcation lines: point Q is stable for all values of ϕ (i.e. for all $(\phi, \mu(\phi))$ on the line of flip bifurcations.

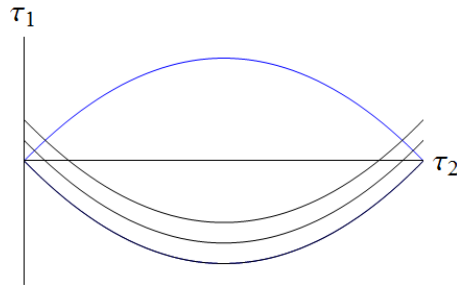


Figure 7: The situation for $\mu = 0, \phi = 0.25\pi$: the whole lower arc consists of unstable equilibria.

the first nontrivial normal form at $\lambda = -1$, thus at $\phi = \frac{3\pi}{4}$, the whole upper arc of the phase space consisted of equilibria. This degeneracy, which is the motivation for the present work, is resolved by the second nontrivial normal form, as is shown by theorem 2. By the above we can also conclude that at point $(Y, 0)$ in the parameter plane (ϕ, μ) , a flip bifurcation occurs. To summarize, flip bifurcations occur apart from $(\mu = 0, \phi = \frac{\pi}{4})$ and where the single point of $V_{\pm 1}$ bifurcates.

5 The singular point $\tau = (0, 0, 0)$

We now set $\mu = 0$ and look at the stability of $\tau = (0, 0, 0)$, which we also call point P. There are again three cases:

1. The level set of the Hamiltonian passes outside the phase space, hence the modulus of its slope at P is larger than the modulus of the slope of the phase space at P.
2. The level set of the Hamiltonian passes inside the phase space, hence the modulus of its slope at P is smaller than the modulus of the slope of the phase space at P.
3. The slope of the level set of the Hamiltonian is equal to the slope of the phase space at P.

We will see that if we go from $|\mu| \neq 0$ to $\mu = 0$, in one of the first two cases point P bifurcates. So solving the last equation will only give the endpoints of these bifurcation lines. Recall that from [4] we already know that some of these solutions will be Hamiltonian Hopf bifurcations. What happens is that when crossing the bifurcation value, a centre turns into a saddle. So in the three-degree-of-freedom system the periodic orbit undergoes a Hamiltonian Hopf bifurcation.

5.1 The bifurcation lines concerning $\tau = (0, 0, 0)$

At $\tau = (0, 0, 0)$ the phase space can be approximated by the cone

$$\tau_1 = \pm\tau_2.$$

Filling in $\tau = (0, 0, 0)$ and $\mu = 0$ in (16) gives the slope

$$-\frac{b_1}{a_1}$$

of the level set of the Hamiltonian at P. These two slopes should be equal, so we want to solve

$$a_1 = \pm b_1$$

for ϕ . We find three solutions independent of δ

$$\phi = \frac{\pi}{4}, \phi = \arctan \frac{1}{2}, \phi = \arctan \frac{5}{2},$$

which correspond to $\lambda = \frac{1}{2}$, $\lambda = 1$ and $\lambda = \frac{5}{2}$. These were the ones that also appeared for the first nontrivial normal form. There is one more solution of the equation $b_1 = -a_1$, depending on δ , with values slightly smaller than $\phi = \frac{3\pi}{4}$. We will refer to this point as point $(X, 0)$ in the (ϕ, μ) -parameter plane.

Theorem 3. *X decreases when δ increases, in a small neighbourhood around $(\phi = \frac{3\pi}{4}, \delta = 0)$. When $\delta \downarrow 0$ this point goes to $\phi = \frac{3\pi}{4}$ (so to $\lambda = -1$).*

Proof. Again we apply the implicit function theorem. The point of interest is a solution of

$$a_1 = -b_1.$$

So we write

$$h(\phi, \delta) = a_1 + b_1.$$

Note that $h(\phi, \delta)$ is a C^1 function on \mathbb{R}^2 . We know that $h(\frac{3\pi}{4}, 0) = 0$. Also

$$\frac{\partial h}{\partial \phi} \Big|_{(\frac{3\pi}{4}, 0)} = 30.0002.$$

Hence the implicit function theorem is applicable: there is a C^1 function $\phi = \phi(\delta)$ defined on an open interval around $\delta = 0$ such that $\phi(0) = \frac{3\pi}{4}$ and

$$\frac{d\phi}{d\delta}(0) = -\frac{\frac{\partial h}{\partial \delta} \Big|_{(\frac{3\pi}{4}, 0)}}{\frac{\partial h}{\partial \phi} \Big|_{(\frac{3\pi}{4}, 0)}}.$$

Computing this derivative gives

$$\frac{d\phi}{d\delta}(0) = -\frac{756}{30.002} < 0.$$

Indeed we see that increasing δ gives a smaller value of X on a small neighbourhood around $(\frac{3\pi}{4}, 0)$. Moreover, if we take $\delta \downarrow 0$ then X goes to $\phi = \frac{3\pi}{4}$. \square

We have also computed the value of X for several values of δ . The result can be seen in table 3.

	$a_1 = -b_1$
$\delta = 0$	$\phi \approx 2.356194 = \arctan(-1) = \frac{3\pi}{4}$
$\delta = 10^{-7}$	$\phi \approx 2.356192$
$\delta = 10^{-6}$	$\phi \approx 2.356169$
$\delta = 10^{-5}$	$\phi \approx 2.355943$

Table 3: The numerical values of X for different values of δ .

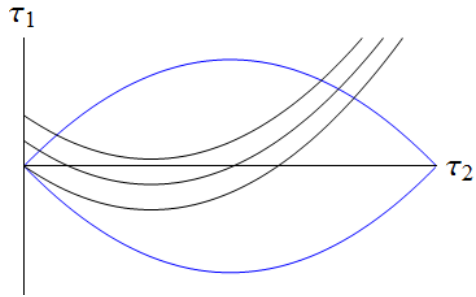
5.2 The stability of $\tau = (0, 0, 0)$

To determine the stability of point P we follow the same approach as in section 4.4. In figure 8 the different situations are shown. If the level set of the Hamiltonian passes outside the phase space, point P is stable: if we move the starting point closer to P, the whole trajectory is closer to P. If the level set of the Hamiltonian passes inside the phase space, point P is unstable. In this case point P bifurcates since for sufficiently small $|\mu| \neq 0$ there are no equilibria close to $(|\mu|, 0)$, but there are nearby orbits with large period. Thus in the case that P is unstable, going from $|\mu| \neq 0$ to $\mu = 0$ a new equilibrium appears: point P. This gives the bifurcation lines $\{(\lambda, 0) \mid \lambda < X\}$, $\{(\lambda, 0) \mid \frac{1}{2} < \lambda < 1\}$, and $\{(\lambda, 0) \mid \lambda > \frac{5}{2}\}$.

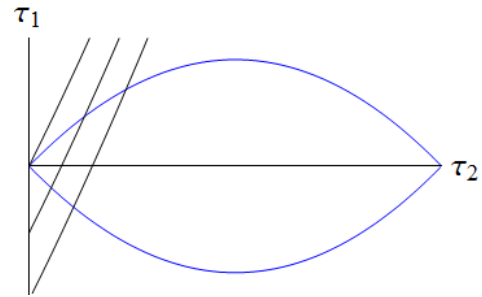
If the slope of the level set of the Hamiltonian coincides with the slope of the phase space at P, we should again look at the second derivative. But here we only have four cases in which we have to check the stability of P: $\phi = \frac{\pi}{4}$, $\phi = \arctan \frac{1}{2}$, $\phi = \arctan \frac{5}{2}$ and point $\phi = X$. Notice that we already know that if $\phi = \frac{\pi}{4}$ then point P is unstable, see figure 7. From figure 8 we can read off the stability of P in the other cases: if $\phi = \arctan(0.5)$ or $\phi = \arctan(2.5)$ then P is stable, if $\phi = X$ then point P is unstable.

At $\lambda = 1$ the original system (1) is integrable and as we already saw in section 4.4 for $\mu = 0$ there is an infinite number of equilibria on the lower arc of the phase space. This degeneracy holds for all higher order normal forms. At $\lambda = \frac{1}{2}$ and $\lambda = \frac{5}{2}$ a Hamiltonian Hopf bifurcation of the supercritical type occurs, as proven in [4]. Note that it is already known that this exactly happens at $\lambda = \frac{1}{2}$ for the normal form of all orders, but for $\lambda = \frac{5}{2}$ it is not known if the Hamiltonian Hopf bifurcation stays at this exact value or will shift a bit, depending on δ , for the normal form of higher orders. At X another Hamiltonian Hopf bifurcation of the subcritical type happens, as is

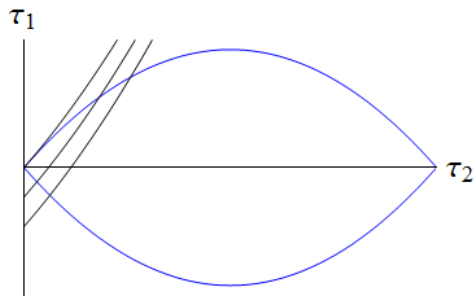
proven in [8].



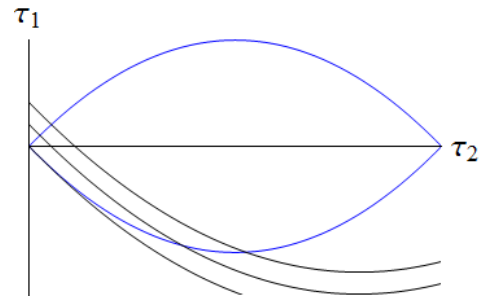
(a) The Hamiltonian passes inside the phase space, P is unstable.



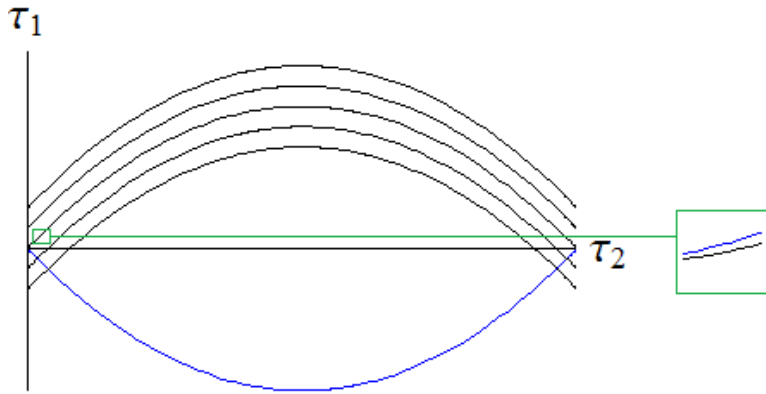
(b) The Hamiltonian passes outside the phase space so P is stable.



(c) The situation for $\phi = \arctan(0.5)$, P is stable.



(d) The situation for $\phi = \arctan(2.5)$, P is stable.



(e) The situation at point X (the value depends on δ and can be found in table 3), P is unstable as we can see from the small area we zoomed in at.

Figure 8: The different situations for the stability of $\tau = (0, 0, 0)$.

6 The equilibria at regular points

To study the equilibria at regular points we are going to work in nodal-Lissajous variables, which simplifies the equations we obtain a lot. Furthermore, we will work with the second nontrivial normal form before the rescaling of τ_1, τ_2 and τ_3 was done, $\bar{\mathcal{H}}_\epsilon^{a,b;\lambda}$ on the phase space $V_{a,b}$, for reasons that will become clear during the calculation. We also need two new concepts: the Poisson bracket and Liouville's theorem.

Definition 2. *Let E be an open subset of \mathbb{R}^{2n} described by coordinates $(x, p) = (x_1, \dots, x_n, p_1, \dots, p_n)$. The Poisson bracket of two functions $F, G: E \subset \mathbb{R}^{2n} \rightarrow \mathbb{R}$ is another function $H: E \subset \mathbb{R}^{2n} \rightarrow \mathbb{R}$ such that*

$$H = \{F, G\} = \sum_{i=1}^n \left(\frac{\partial F}{\partial x_i} \frac{\partial G}{\partial p_i} - \frac{\partial F}{\partial p_i} \frac{\partial G}{\partial x_i} \right).$$

After reduction of our system the Poisson bracket on the phase space $V_{a,b}$ has turned into

$$\{f, g\} = 2(\nabla f \times \nabla g | \nabla R_{a,b}), \quad (21)$$

where $(\cdot | \cdot)$ denotes the standard inner product and

$$R_{a,b}(\tau) = \tau_1^2 + \tau_3^2 - (\tau_2 - 2b)^2(\tau_2^2 - 4a^2). \quad (22)$$

Liouville's Theorem. *Suppose \mathcal{H} is a Hamiltonian function and the function F does not depend on t . Then, along the flow: $\dot{F} = \{F, \mathcal{H}\}$.*

We can now set up the differential system in τ_i . Using the definition of the Poisson bracket and Liouville's theorem we find for $i \in \{1, 2, 3\}$ that

$$\begin{aligned} \dot{\tau}_i &= \{\tau_i, \bar{\mathcal{H}}_\epsilon^{a,b;\lambda}(\tau)\} \\ &= \sum_{j=1}^3 \left(\frac{\partial \tau_i}{\partial x_j} \frac{\partial \bar{\mathcal{H}}_\epsilon^{a,b;\lambda}(\tau)}{\partial p_j} - \frac{\partial \tau_i}{\partial p_j} \frac{\partial \bar{\mathcal{H}}_\epsilon^{a,b;\lambda}(\tau)}{\partial x_j} \right) \\ &= \sum_{j=1}^3 \left(\frac{\partial \tau_i}{\partial x_j} \frac{\partial \tau_j}{\partial p_j} - \frac{\partial \tau_i}{\partial p_j} \frac{\partial \tau_j}{\partial x_j} \right) \frac{\partial \bar{\mathcal{H}}_\epsilon^{a,b;\lambda}(\tau)}{\partial \tau_j} \\ &= \sum_{j=1}^2 \{\tau_i, \tau_j\} \frac{\partial \bar{\mathcal{H}}_\epsilon^{a,b;\lambda}(\tau)}{\partial \tau_j}, \end{aligned} \quad (23)$$

$\{\tau_i, \tau_j\}$	τ_1	τ_2	τ_3
τ_1	0	$4\tau_3$	$8(\tau_2 - 2b)(\tau_2^2 - b\tau_2 - 2a^2)$
τ_2	$-4\tau_3$	0	$4\tau_1$
τ_3	$-8(\tau_2 - 2b)(\tau_2^2 - b\tau_2 - 2a^2)$	$-4\tau_1$	0

Table 4: The Poisson brackets for the τ_i . The τ_i on the left must be put in the left side of the bracket, the τ_j on the top must be placed in the right side of the bracket.

where in the last step we used that $\bar{\mathcal{H}}_\epsilon^{a,b;\lambda}(\tau)$ only depends on the variables τ_1 and τ_2 but not on τ_3 . We can calculate the Poisson brackets of τ_1, τ_2, τ_3 by using the Poisson bracket (21). Suppose we want to know $\{\tau_1, \tau_2\}$. Since

$$\nabla_{\tau_1} \times \nabla_{\tau_2} = \begin{pmatrix} 0 \\ 0 \\ 1 \end{pmatrix}$$

we find that

$$\{\tau_1, \tau_2\} = 2 \frac{\partial R_{a,b}(\tau_1, \tau_2, \tau_3)}{\partial \tau_3} = 4\tau_3.$$

Similarly we can compute the other brackets, obtaining the values shown in table 4. By using (23) and the Poisson brackets found for τ_1, τ_2 and τ_3 we can compute the differential system, resulting in

$$\begin{aligned} \dot{\tau}_1 = & 4\tau_3 \left[4b(5 - 6\lambda - 4\lambda^2) - 2(5 - 12\lambda - 3\lambda^2)\tau_2 \right. \\ & + \frac{2\delta}{b} [-4a^2\lambda^2(43 - 372\lambda + 369\lambda^2) \\ & + 4b^2(705 - 720\lambda - 251\lambda^2 - 972\lambda^3 - 172\lambda^4) \\ & + 2\lambda(1 - \lambda)(41 - 61\lambda - 606\lambda^2)\tau_1 \\ & \left. - 12b(235 - 480\lambda + 63\lambda^2 - 588\lambda^3 + 300\lambda^4)\tau_2 \right. \\ & \left. - 15(1 - \lambda)(47 - 97\lambda - 9\lambda^2 - 201\lambda^3)\tau_2^2 \right] \\ \dot{\tau}_2 = & -8\lambda\tau_3 \left[1 - 6\lambda + \frac{2\delta}{b} [2b(41 - 42\lambda - 656\lambda^2 - 48\lambda^3) \right. \\ & \left. - (1 - \lambda)(41 - 61\lambda - 606\lambda^2)\tau_2] \right] \end{aligned}$$

and

$$\begin{aligned}
\dot{\tau}_3 = & 8 \left[4a^2\lambda(1-6\lambda)(\tau_2-2b) - 2b(5-6\lambda-4\lambda^2)\tau_1 + (5-12\lambda-3\lambda^2)\tau_2\tau_1 \right. \\
& - 4b^2\lambda(1-6\lambda)\tau_2 + 6b\lambda(1-6\lambda)\tau_2^2 - 2\lambda(1-6\lambda)\tau_2^3 \\
& + \frac{2\delta}{b}[-16a^2b^2\lambda(41-42\lambda-656\lambda^2-48\lambda^3) \\
& - 2b^2(705-720\lambda-251\lambda^2-972\lambda^3-172\lambda^4)\tau_1 \\
& + 2a^2\lambda^2(43-372\lambda+369\lambda^2)\tau_1 \\
& + \lambda(1-\lambda)(41-61\lambda-606\lambda^2)\tau_1^2 \\
& - 8b^3\lambda(41-42\lambda-656\lambda^2-48\lambda^3)\tau_2 \\
& + 8a^2b\lambda(82-144\lambda-1201\lambda^2+558\lambda^3)\tau_2 \\
& + 6(235-480\lambda+43\lambda^2-588\lambda^3+300\lambda^4)\tau_1\tau_2) \\
& + 4b^2\lambda(164-228\lambda-2513\lambda^2+462\lambda^3)\tau_2^2 \\
& - 4a^2\lambda(41-102\lambda-545\lambda^2+606\lambda^3)\tau_2^2 \\
& - \frac{15}{2}(1-\lambda)(47-97\lambda-9\lambda^2-201\lambda^3)\tau_1\tau_2^2 \\
& - 2b\lambda(205-390\lambda-2947\lambda^2+1722\lambda^3)\tau_2^3 \\
& \left. + 2\lambda(1-\lambda)(41-61\lambda-606\lambda^2)\tau_2^4 \right]. \tag{24}
\end{aligned}$$

We are looking for places in the parameter plane where the regular equilibria bifurcate. Equilibria are points on the phase space such that $\dot{\tau}_1 = \dot{\tau}_2 = \dot{\tau}_3 = 0$. As explained at the beginning of chapter 3 these equilibria are confined to $\tau_3 = 0$. Notice that we then have $\dot{\tau}_1 = \dot{\tau}_2 = 0$ automatically. Solving $\dot{\tau}_3 = 0$ with the constraints $\tau_3 = 0$ and (22) gives the regular equilibria. Regular equilibria bifurcate whenever the Hamiltonian function (12) touches the meridian section of the phase space (11) in a degenerate way. It is shown in [2] that such a bifurcation must be a centre-saddle bifurcation: two regular equilibria, a saddle and a centre, collide and annihilate each other. Thus we have to look for the existence of multiple roots of (24) with the constraints $\tau_3 = 0$ and (22). To do this, we need one more concept.

Definition 3. Let p_1 and p_2 be two polynomials defined over \mathbb{R} ,

$$\begin{aligned}
p_1(x) &= a_0x^m + a_1x^{m-1} + \dots + a_m, \\
p_2(x) &= b_0x^n + b_1x^{n-1} + \dots + b_n,
\end{aligned}$$

with $a_0 \neq 0$ and $b_0 \neq 0$. Let $\alpha_1, \dots, \alpha_m$ and β_1, \dots, β_n be the roots of respectively

p_1 and p_2 in \mathbb{C} . Then the resultant of p_1 and p_2 is defined as

$$R(p_1, p_2) = a_0^s b_0^n \prod_{i=1}^m \prod_{j=1}^n (\alpha_i - \beta_j).$$

So one can calculate the resultant of two polynomials by first calculating their roots. It turns out that without knowing the roots of the polynomials, the resultant of these polynomials can also be calculated: the resultant is merely a function of the coefficients of the two polynomials. See [6] for the explicit formula. One nice feature of the resultant $R(p_1, p_2)$ of the polynomials p_1 and p_2 is that if $R(p_1, p_2) = 0$ then p_1 and p_2 share at least one root.

Notice that (24) is not a polynomial in τ_2 . We switch to the use of the nodal-Lissajous variables to obtain a polynomial. We recall that after the second reduction, the axial momentum N and energy L have fixed values a and b respectively, while the total momentum G still varies. We make use of the state functions $\mu = a/b$, $c = a/G$, $s = \sqrt{1 - c^2}$, $\eta = G/b$ and $e = \sqrt{1 - \eta^2}$. Notice that s can be expressed in e and μ since

$$\begin{aligned} s^2 &= 1 - c^2 = 1 - \frac{a^2}{G^2} = \frac{G^2 - a^2}{G^2} \\ &= \frac{b^2 - (b^2 - G^2) - a^2}{b^2 - (b^2 - G^2)} \\ &= \frac{1 - \frac{b^2 - G^2}{b^2} - \frac{a^2}{b^2}}{1 - \frac{b^2 - G^2}{b^2}} \\ &= \frac{1 - e^2 - \mu^2}{1 - e^2}. \end{aligned} \tag{25}$$

Our strategy for finding the centre-saddle bifurcation is the following: we first rewrite (24) as a polynomial in the variable e and parameters μ and λ . Once we have done that, we calculate the resultant of this polynomial and its derivative, giving an expression in μ and λ . We then equate this resultant to zero. By doing this we impose that the polynomial and its derivative share at least one root. This gives the centre-saddle bifurcation lines.

We first use the expressions of τ_1 , τ_2 and τ_3 in the nodal-Lissajous variables,

see (10). We can rewrite them using the state functions as

$$\begin{aligned}
\tau_1 &= 2s^2(b^2e^2 + b^2e \cos 2g) - s^4(b + be \cos 2g)^2 \\
\tau_2 &= b - be \cos 2g + (1 - s^2)(b + be \cos 2g) \\
\tau_3 &= 2s^2b^2\eta e \sin 2g,
\end{aligned} \tag{26}$$

in which we can substitute (25) to eliminate s . Recall that the equilibria are confined to $\tau_3 = 0$. Taking $\tau_3 = 0$ we see that there are two cases: $g = 0$ or $g = \frac{\pi}{2}$. If we look at $g = 0$ then the regular equilibria lie on the upper arc, if we take $g = \frac{\pi}{2}$ then they lie on the lower arc. When finding an expression for the centre-saddle bifurcation, the two equilibria that are going to collide need to lie on the same arc. Hence we will split our search in two cases.

6.1 Regular equilibria on the upper arc of the phase space

We take $g = 0$ and substitute (26) into (24). After doing this we eliminate all factors that cannot be zero, since we only want to look at $\dot{\tau}_3 = 0$. In this

way we obtain a polynomial

$$\begin{aligned}
\mathcal{P}_1(e, s) = & -4a^2\lambda + 4b^2\lambda + 24a^2\lambda^2 - 24b^2\lambda^2 + 6b^2\lambda s^2 + 34b^2\lambda^2 s^2 + 5b^2 s^4 \\
& - 10b^2\lambda s^4 - 15b^2\lambda^2 s^4 - 2b^2 e(12\lambda - 2\lambda^2 + 5s^2 - 15\lambda s^2 - 20\lambda^2 s^2 \\
& - 5s^4 + 10\lambda s^4 + 15\lambda^2 s^4) - b^2 s^2 e^2(10 - 24\lambda - 6\lambda^2 - 5s^2 + 10\lambda s^2 \\
& + 15\lambda^2 s^2) \\
& + \delta[-960a^2\lambda^2 + 960b^2\lambda^2 + 1776a^2\lambda^3 - 1776b^2\lambda^3 \\
& + 10464a^2\lambda^4 - 10464b^2\lambda^4 - 328a^2\lambda s^2 + 328b^2\lambda s^2 + 644a^2\lambda^2 s^2 \\
& + 508b^2\lambda^2 s^2 + 5848a^2\lambda^3 s^2 - 2992b^2\lambda^3 s^2 - 6324a^2\lambda^4 s^2 \\
& + 24716b^2\lambda^4 s^2 + 2388b^2\lambda s^4 - 2820b^2\lambda^2 s^4 + 10116b^2\lambda^3 s^4 \\
& - 20964b^2\lambda^4 s^4 + 705b^2 s^6 - 1914b^2\lambda s^6 + 708b^2\lambda^2 s^6 - 6150b^2\lambda^3 s^6 \\
& + 6651b^2\lambda^4 s^6 - e(-344a^2\lambda^2 + 5528b^2\lambda^2 + 2976a^2\lambda^3 - 2592b^2\lambda^3 \\
& - 2952a^2\lambda^4 + 8344b^2\lambda^4 + 328a^2\lambda s^2 + 5432b^2\lambda s^2 - 644a^2\lambda^2 s^2 \\
& - 9556b^2\lambda^2 s^2 - 5848a^2\lambda^3 s^2 + 11920b^2\lambda^3 s^2 + 6324a^2\lambda^4 s^2 \\
& - 41636b^2\lambda^4 s^2 + 1410b^2 s^4 - 8768b^2\lambda s^4 + 7464b^2\lambda^2 s^4 - 30352b^2\lambda^3 s^4 \\
& + 52806b^2\lambda^4 s^4 - 2115b^2 s^6 + 5742b^2\lambda s^6 - 2124b^2\lambda^2 s^6 \\
& + 18450b^2\lambda^3 s^6 - 19953b^2\lambda^4 s^6) + b^2 e^2 s^2(-5432\lambda + 8232\lambda^2 \\
& - 13288\lambda^3 + 21768\lambda^4 - 2820s^2 + 10372\lambda s^2 - 6468\lambda^2 s^2 \\
& + 30356\lambda^3 s^2 - 42720\lambda^4 s^2 + 2115s^4 - 5742\lambda s^4 + 2124\lambda^2 s^4 \\
& - 18450\lambda^3 s^4 + 19953\lambda^4 s^4) + b^2 e^3(-1 + \lambda)s^2(-328\lambda + 488\lambda^2 \\
& + 4848\lambda^3 + 1410s^2 - 2582\lambda s^2 - 758\lambda^2 s^2 - 10878\lambda^3 s^2 \\
& - 705s^4 + 1209\lambda s^4 + 501\lambda^2 s^4 + 6651\lambda^3 s^4)].
\end{aligned} \tag{27}$$

Notice that this equation is homogeneous in a and b : terms have either got a factor b^2 or a factor a^2 . This is why we used the Hamiltonian function before scaling τ_1 , τ_2 and τ_3 : otherwise (27) would not be homogeneous in a and b . We are interested in the case $\mathcal{P}_1 = 0$ so we can divide the right hand side of (27) by b^3 . Effectively we scale b to one and replace a with μ . Hence we get rid of a and b and obtain an expression in the variables e and s and parameters λ and μ . Moreover we can eliminate s . Since in (27) the variable s only enters through even powers of s we can use (25) to eliminate s and still have a polynomial equation. After simplifying and omitting the

common factors of this equation we obtain the following polynomial

$$\begin{aligned}
\mathcal{P}_1(e) = & -(-1+e)[5(1+\lambda)(-1+\mu)(1+\mu)(1-\lambda-\mu^2+3\lambda\mu^2) \\
& + 2e(5+7\lambda-12\lambda^2-5\mu^2+5\lambda\mu^2+10\lambda^2\mu^2) \\
& + 42e^2(-1+\lambda)\lambda + e^3(-1+\lambda)(10-32\lambda+e(-5+9\lambda))] \\
& + \delta[(\mu^2-1)(705+802\lambda-644\lambda^2-802\lambda^3-61\lambda^4-1410\mu^2 \\
& + 1112\lambda\mu^2+2048\lambda^2\mu^2+8032\lambda^3\mu^2+1338\lambda^4\mu^2+705\mu^4-1914\lambda\mu^4 \\
& + 708\lambda^2\mu^4-6150\lambda^3\mu^4+6651\lambda^4\mu^4) + 2e(705+2406\lambda-310\lambda^2 \\
& - 2490\lambda^3-311\lambda^4-1410\mu^2-1932\lambda\mu^2+4044\lambda^2\mu^2+8532\lambda^3\mu^2 \\
& + 1726\lambda^4\mu^2+705\mu^4-474\lambda\mu^4-1142\lambda^2\mu^4-5850\lambda^3\mu^4 \\
& + 1281\lambda^4\mu^4) + e^2(705-8822\lambda-5892\lambda^2+11510\lambda^3+2499\lambda^4 \\
& - 1410\mu^2+10900\lambda\mu^2-9452\lambda^2\mu^2-7324\lambda^3\mu^2-3034\lambda^4\mu^2 \\
& + 705\mu^4-2078\lambda\mu^4+944\lambda^2\mu^4-2482\lambda^3\mu^4+2751\lambda^4\mu^4) \\
& + 4e^3(-705+802\lambda+4222\lambda^2-3070\lambda^3-1249\lambda^4+705\mu^2 \\
& - 2242\lambda\mu^2+1352\lambda^2\mu^2-302\lambda^3\mu^2+327\lambda^4\mu^2) \\
& - e^4(-705-7218\lambda+18772\lambda^2-5550\lambda^3-5299\lambda^4+705\mu^2 \\
& - 2242\lambda\mu^2+1352\lambda^2\mu^2-302\lambda^3\mu^2+327\lambda^4\mu^2) \\
& - 2e^5(-1+\lambda)(705-3305\lambda+1537\lambda^2+1431\lambda^3) \\
& + 3e^6(-1+\lambda)(235-567\lambda+77\lambda^2+207\lambda^3)].
\end{aligned}$$

Recall that the centre-saddle bifurcation happens whenever \mathcal{P}_1 has a multiple root. That is, \mathcal{P}_1 and its derivative with respect to e has got a common root. Hence we calculate the resultant $r(\lambda, \mu)$ of \mathcal{P}_1 and its derivative with respect to e using Mathematica. After computation we can simplify the resultant since we want to solve $r(\lambda, \mu) = 0$, so after factorizing we cancel the factors that cannot be zero. This results in a polynomial of degree 39 in λ and degree 16 in μ , too large to write down explicitly here. We point out that μ only enters through even powers, which we expected since the bifurcation plane is symmetric under reflection of μ . There is no explicit analytic solution of $r(\lambda, \mu) = 0$ but we can draw the resulting line using a contour plot in Mathematica. The result is shown in figure 9.

For the first nontrivial normal form the centre-saddle bifurcation line goes through $(\lambda = -1, \mu = 0)$. For the second nontrivial normal form we see that

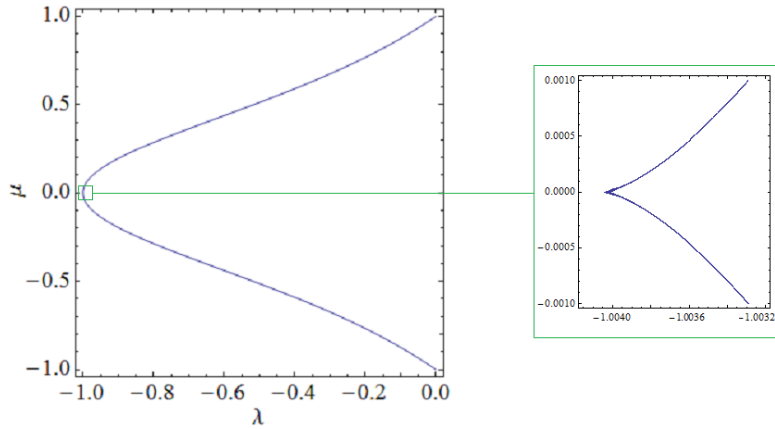


Figure 9: The centre-saddle bifurcation. The little area we zoomed in at shows that the centre-saddle bifurcation does not go through $(\lambda = -1, \mu = 0)$ but at a point slightly more to the left, depending on δ . This picture was made for the situation $\delta = 10^{-5}$.

this is not the case,

$$r(-1, 0) = 61896565413399557302124544 \delta^5 (1 + 372 \delta + 42912 \delta^2 + 1102464 \delta^3 - 47672064 \delta^4 + 331195392 \delta^5),$$

so for small enough $\delta > 0$ (to be precise, $0 < \delta < \frac{1}{12}$) the resultant at $(\lambda = -1, \mu = 0)$ is non-zero. The curve $r(\lambda, \mu) = 0$ goes through $\mu = 0$ at a point slightly smaller than $\lambda = -1$. It also appears that the curve is not smoothly going through point X , as expected from a subcritical Hamiltonian Hopf bifurcation.

6.2 Regular equilibria on the lower arc of the phase space

We now take $g = \frac{\pi}{2}$. We follow the same strategy as before and rewrite (24) as a polynomial with variable e and with coefficients depending on parameters λ and μ . We then compute the resultant of this polynomial and its derivative. We obtain $s(\lambda, \mu)$ and it turns out that $s(\lambda, \mu) = -r(\lambda, \mu)$. All the curves that are a solution of $s(\lambda, \mu) = 0$ in the (λ, μ) -plane have to be discarded, since they are not part of the domain of e : $0 < e < \sqrt{1 - \mu^2}$.

7 The bifurcation diagram

In figure 10 part of the bifurcation diagram of the second nontrivial normal form can be seen. We will see in section 8 that global bifurcations occur in region 2, these are the only bifurcations not portrayed in figure 10. We have pictured the equilibria (and their stability) for each region in the diagram by representing the phase space by the planar sections of the lemons or turnips, but we have not illustrated the fact that V_μ decreases to a point as $|\mu| \rightarrow 1$. Note that the bifurcation diagram is symmetric with respect to the λ axis.

The lines of Hamiltonian flip bifurcations are lines B and F, see section 4 for the calculation of the equations of these lines, which correspond to the single circle in figure 2. We will describe what happens with the flow of the second nontrivial normal form on the phase space when crossing the line of Hamiltonian flip bifurcations. In region 6 there is a stable equilibrium at the upper arc, a stable equilibrium at the lower arc and point Q is unstable. Getting closer to the line F the equilibrium at the lower arc gets closer to point Q. At line F the equilibrium at the lower arc collides with point Q, which becomes stable. In region 5 there are only two equilibria: one on the upper arc, which remained stable the whole time, and point Q that became stable during the transition from region 6 to region 5. See figure 11. Going from region 1 to 3 the same thing happens, but now on the upper arc of the phase space. Recall that line F touches $\mu = \pm 1$ at a value slightly larger than $\lambda = 6$, depending on δ , see table 1. The new region that emerges for $\lambda > 6$, between the curve F and $\mu = \pm 1$, is equivalent to region 3. Crossing from region 6 to this new region, the centre on the upper arc is annihilated by point Q, turning Q from unstable into stable. Going from region 2 to 4 can be seen in figure ?? and will be discussed in section 8.

The line of the centre-saddle bifurcations is line C, see section 6 for the calculation of the equation of this line. First we will describe the crossing from region 4 to 3. In region 4 there are four equilibria: a centre at the lower arc (nothing will happen with this equilibrium during the crossing), a centre at the left side of the upper arc and a saddle on the right side of the upper arc. Point Q is stable. When moving closer to line C, but staying in region 4, the centre is moving closer to the saddle. At line C the saddle has annihilated the centre and has become a parabolic equilibrium. In region 3 there is no longer a regular equilibrium on the upper arc of the phase space.

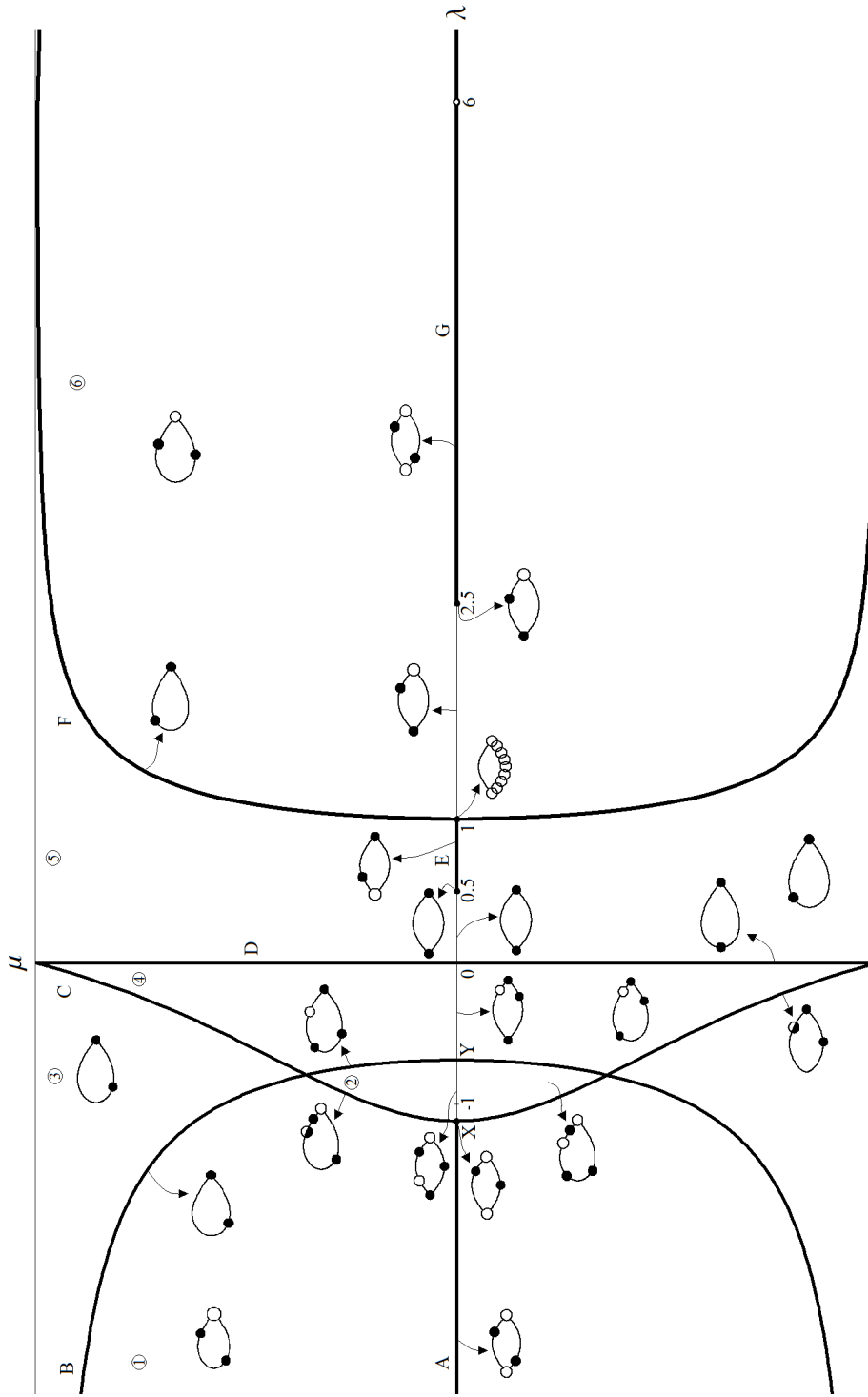


Figure 10: The bifurcation diagram and meridian sections $\tau_3 = 0$ of the lemons and turnips. Black circles are stable points (for regular equilibria centres) while white circles are unstable points (for regular equilibria saddles) and parabolic equilibria are black-white circles. The global bifurcations that occur in region 2 are not shown, see for this section 8. Note that the diagram is not to scale for $\lambda \in [X, Y]$, otherwise region 2 would not be visible.

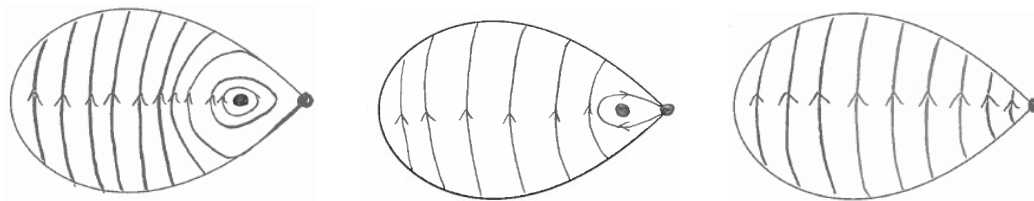


Figure 11: View from below on the phase space. The picture on the left shows the situation in region 6, the one in the middle is the situation when still being in region 6 but moving closer to line F. The picture on the right shows the situation at line F and in region 5.

At the lower arc there is still a centre and point Q is remained stable during the transition. See figure 12 for the view from the upper part of the phase space. The transition from region 2 to 1 is quite similar to going from 4 to 3: although there is one more equilibrium present in region 2 compared to region 4, it does not interact in the bifurcation. In region 2 point Q is unstable, there are three regular equilibria on the upper arc which are from left to right a centre, a saddle and again a centre. There is also a centre on the lower arc of the phase space. When moving closer in region 2 to line C, the most left centre on the upper arc moves to the saddle. On C they collide, forming a parabolic equilibrium and in region 1 they are gone. The other centre at the upper arc is still there though, as well as the one at the lower arc, and point Q remained unstable. See figure ?? in chapter 8.

Bifurcation line D is the line $\lambda = 0$. In region 4 there are four equilibria, as described before. When λ tends to zero, the centre on the upper arc moves to $\tau = (0, |\mu|, 0)$. The saddle on the upper arc and the centre on the lower arc both move to point Q. When $\lambda = 0$ these three points collide at Q, which remains stable. The other centre reaches point P. After crossing line D the centre moves back from point P to the right (on the upper arc) and point Q is still stable. See figure 13. Since three points collide on line D, this bifurcation looks very degenerate. This is due to the integrability of (1) at $\lambda = 0$ and occurs for every normal form, see [9] for more details.

Bifurcation line A is the line $\{(\lambda, 0) \mid \lambda < X\}$, where the value of X depends on δ but is always slightly smaller than -1 (see table 3). Bifurcation line G is the line $\{(\lambda, 0) \mid \lambda > \frac{5}{2}\}$. At lines A and G there are four equilibria:

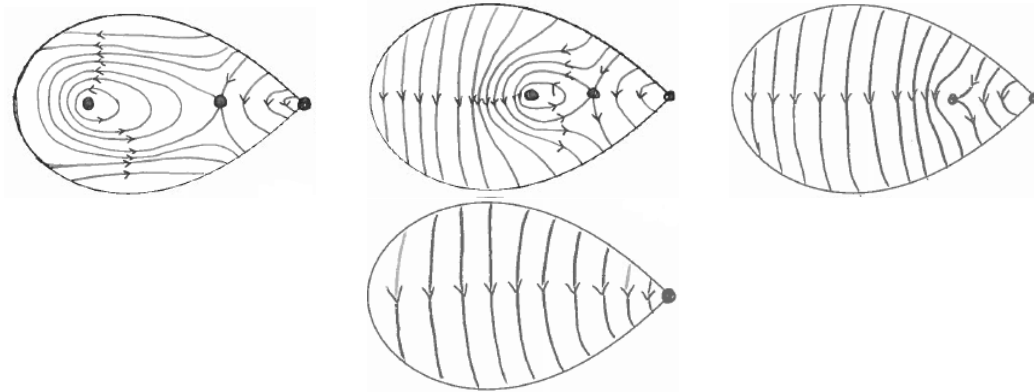


Figure 12: The view on the phase space from the top. The picture on the left shows the situation in region 4, the one to the right is the situation when still being in region 4 but moving closer to line C. The picture on the right shows the situation at line C and the bottom picture shows the situation in region 3.

both $\tau = (0, 0, 0)$ and $\tau = (0, 1, 0)$ are unstable and on each arc there is one centre. When moving from line A into region 1, or from line G into 5, point P disappears, the other equilibria stay the same.

Bifurcation line E is the line $\{(\lambda, 0) \mid \frac{1}{2} < \lambda < 1\}$. At this line point P is unstable, point Q is stable and there is a centre at the upper arc. Going from segment E into region 5 the unstable equilibrium at $\tau = (0, 0, 0)$ disappears, the other two stable equilibria remain.

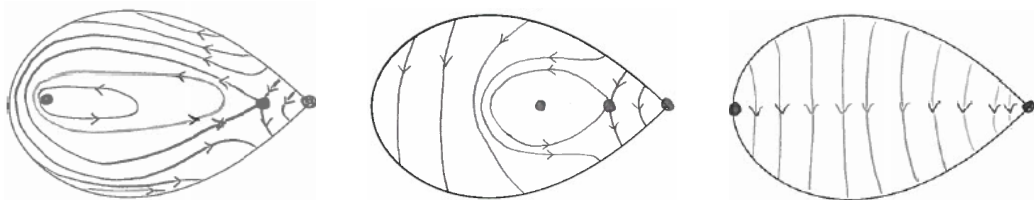


Figure 13: The view on the phase space from the top. On the left the situation in region 4 is shown, in the middle we see what happens when still being in region 4 but very close to line D. On the right the situation at line D is shown.

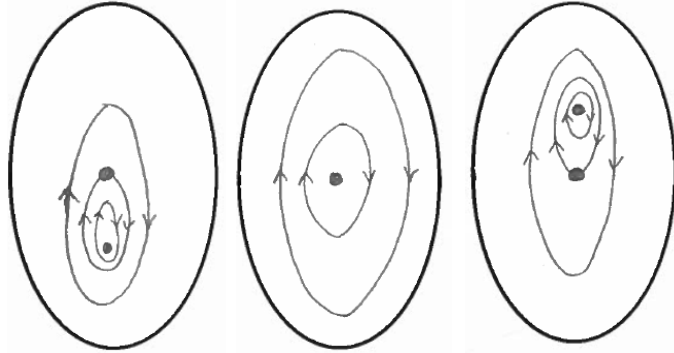


Figure 14: The view on the phase space from the left. On the left the situation at line G is shown. The picture in the middle shows the situation for $\lambda = \frac{1}{2}$, which is exactly the same as for $(\lambda, \mu) = (\frac{5}{2}, 0)$. On the right the situation at line E is shown.

The supercritical Hamiltonian Hopf bifurcations occur at $(\lambda, \mu) = (\frac{1}{2}, 0)$ and $(\lambda, \mu) = (\frac{5}{2}, 0)$. At $(\lambda, \mu) = (\frac{1}{2}, 0)$ point P and Q are stable, no more equilibria are present. When increasing λ , but keeping $\mu = 0$, point P becomes unstable and a centre at the upper arc appears, see figure 14. When decreasing λ , but not changing μ , nothing happens. When changing μ , from point P emerges a centre on the upper arc of the phase space. At $(\lambda, \mu) = (\frac{5}{2}, 0)$ point P is stable but Q is unstable, and a centre at the upper arc is present. When increasing λ point P becomes unstable and a centre on the lower arc appears from it, see figure 14. When decreasing λ nothing happens. When changing μ point P becomes a centre on the lower arc. At $(\lambda, \mu) = (X, 0)$ a subcritical Hamiltonian Hopf bifurcation occurs. When increasing λ point P becomes stable, when decreasing λ point P stays unstable.

In case $(\lambda, \mu) = (1, 0)$ the whole lower arc consists of unstable equilibria, as we already saw in figure 7. This is the same degeneracy that was encountered in the first nontrivial normal form, and persists throughout all normal forms of higher order, as is shown in [7].

8 Global bifurcations

Global bifurcations occur whenever two (or more) unstable equilibria have the same energy. There are two situations in which there are two unstable equilibria present, see figure 10. If $(\lambda, \mu) \in A$ or $(\lambda, \mu) \in G$ both singular points of the phase space are unstable. The energy of the singular point $\tau = (0, 0, 0)$ is 0, the energy of the singular point $\tau = (0, 1, 0)$ is $b_1 + c + d$, see (13). Solving the equation $b_1 + c + d = 0$ gives no solution for $(\lambda, \mu) \in A$ or $(\lambda, \mu) \in G$. So in this case no global bifurcations occur.

The other situation in which two unstable equilibria are present is in region 2, the region between the line of centre-saddle bifurcations and the line of flip bifurcations. Here the singular point $\tau = (0, 1, 0)$ is unstable and a saddle is present at the upper arc of the phase space. Hence global bifurcations may occur. From [1] we know that at $\mu = 0$ there are two values of λ such that a global bifurcation occurs, one of which is $\lambda = -1$. From [5] we know that at $\lambda = -1$, when the Hamiltonian reduces to the Hénon-Heiles family, there is only one value of μ such that a global bifurcation occurs, namely $\mu = 0$. We will investigate for the whole region 2 if a global bifurcation occurs.

The energy value of the singular point $\tau = (0, 1, 0)$ is

$$h_1 = b_1 + \mu^2 b_2 + c + d,$$

see (13). The energy value of the saddle $\tau = (\tau_1, \tau_2, 0)$ is

$$h_2 = (b_1 + \mu^2 b_2)\tau_2 + c\tau_2^2 + d\tau_2^3 + (a_1 + a_2\tau_2)(1 - \tau_2)\sqrt{\tau_2^2 - \mu^2},$$

where we have taken a plus-sign in (13) since the saddle occurs on the upper arc. We now have two conditions to find for which (λ, μ) the two points have the same energy:

1. $h_1 - h_2 = 0$
2. The point $\tau = (\tau_1, \tau_2, 0)$ is an equilibrium point.

The first condition gives the following equation

$$0 = (b_1 + \mu^2 b_2)(1 - \tau_2) + c(1 - \tau_2^2) + d(1 - \tau_2^3) + (a_1 + a_2\tau_2)(\tau_2 - 1)\sqrt{\tau_2^2 - \mu^2}$$

which, since $\tau = (\tau_1, \tau_2, 0)$ is a regular point so $\tau_2 \neq 1$, can be simplified to

$$(b_1 + \mu^2 b_2) + c(1 + \tau_2) + d(1 + \tau_2 + \tau_2^2) = (a_1 + a_2 \tau_2) \sqrt{\tau_2^2 - \mu^2}. \quad (28)$$

Using (17) the second condition can be written as

$$\begin{aligned} & \mu^2(a_1 - a_2) + (a_1 + 2\mu^2 a_2)\tau_2 - 2(a_1 - a_2)\tau_2^2 - 3a_2\tau_2^3 \\ & = -\sqrt{\tau_2^2 - \mu^2}(b_1 + \mu^2 b_2 + 2c\tau_2 + 3d\tau_2^2). \end{aligned} \quad (29)$$

We want to solve for which (λ, μ) in region 2 both condition 1 and condition 2 are satisfied. Notice that solving (29) for $\mu = 0$ and $\lambda = -1$ gives the equilibrium points $\tau_2 = \frac{1}{4}$ and $\tau_2 = \frac{3}{4}$, independent of $\delta > 0$. If we plug $\tau_2 = \frac{1}{4}$ (and $\mu = 0$ and $\lambda = -1$) into (28) we see that condition 2 is met. So we have found one solution, independent of $\delta > 0$, where a global bifurcation takes place: $(\lambda = -1, \mu = 0)$. This is due to the \mathbb{Z}_3 -symmetry of the original Hénon-Heiles system.

By taking the square of both (28) and (29) we obtain two polynomial equations which we want to reduce to an equation in μ and λ . To do this we could use the resultant and look for zeros of the resultant. It turns out that the resultant is so large that looking numerically for zeros is very time-consuming. Hence we choose to not use the resultant and numerically solve for which (λ, μ) in region 2 both condition 1 and condition 2 are satisfied. Our approach is the following: first we fix the value of δ . Then we know the values of X and Y and thus the interval λ in region 2 lies into. We split this interval into smaller intervals. We can do the same for μ . For every grid point we solve (29) for τ_2 and use this to calculate $h_1 - h_2$. We are interested for which parameter values the sign of $h_1 - h_2$ changes, since that means that a global bifurcation has taken place. For the case $\delta = 10^{-6}$ this gave figure 15. Notice that we indeed see that at $\lambda = -1$ only at $\mu = 0$ a global bifurcation takes place. We also confirmed that for $\mu = 0$ there is another global bifurcation occurring, at a point smaller than $\lambda = -1$, as in [1]. Region 2 is separated into two regions named $2a$ and $2b$ (note that $2a$ is not connected). The flow of the Hamiltonian on the phase space is shown in figure 15 for all cases. At the global bifurcation the energy of the saddle and point Q are equal. In region $2a$ the energy of the saddle is larger than the energy of point Q. In region $2b$ the energy of the saddle is smaller than the energy of point Q.

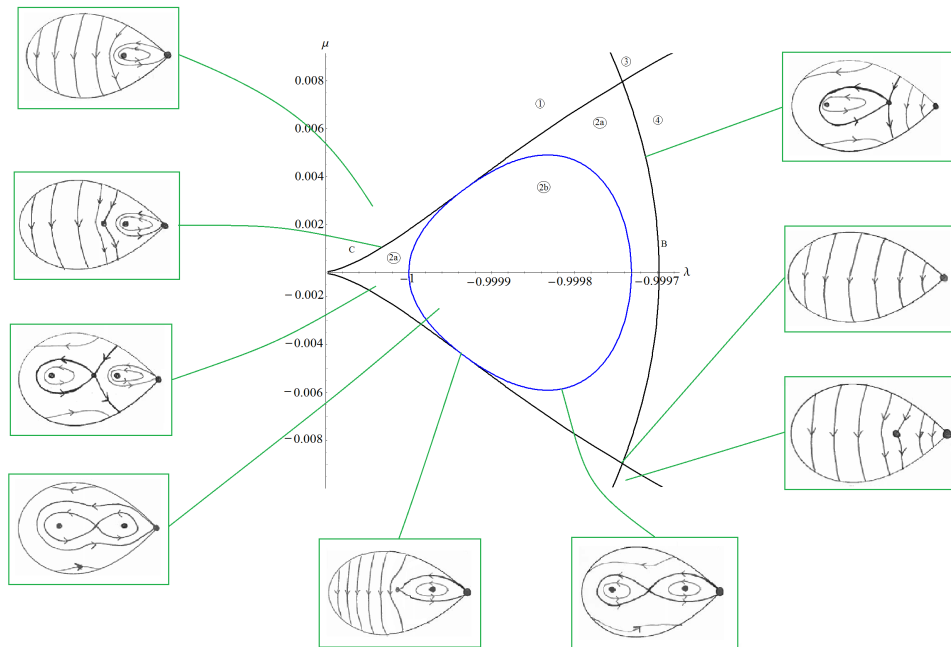


Figure 15: The global bifurcation line is the blue line. The black lines are the lines B (the centre-saddle bifurcations) and C (the flip bifurcations), regions 1, 3 and 4 are as before. We see that region 2 is divided by the global bifurcation into two pieces, region $2a$ and region $2b$. For this figure we have taken $\delta = 10^{-6}$.

It seems from figure 15 that the global bifurcation touches bifurcation line C at one point $\mu > 0$. Since we used numerical methods to obtain the figure we can't confirm this analytically. We do see that going directly from region $2b$ to 1 is impossible. If we go from region 2 to 1, the centre at the left side of the saddle moves towards the saddle. At line C these two collide and form a parabolic equilibrium. At line C the energy of the parabolic equilibrium is higher or equal to the energy of point Q. In region $2b$ the energy of the saddle is lower than that of point Q. So going from $2b$ to 1 requires the energy of the saddle to rise and become at least equal to the energy of point Q, hence we have to cross the global bifurcation line when going from region $2b$ to 1. This does however not exclude that the global bifurcation line touches with line C since we only require the saddle to have an energy at least equal to the energy of point Q.

9 Conclusion

In this thesis we studied the dynamics of the second nontrivial normal form of an axially symmetric perturbation of the isotropic harmonic oscillator.

We have seen that, similar to the case of the first nontrivial normal form, flip bifurcations occur. At $(\lambda = \frac{1}{2}, \mu = 0)$ and $(\lambda = \frac{5}{2}, \mu = 0)$ a Hamiltonian Hopf bifurcation occurs. We have encountered a degeneracy of the second nontrivial normal form at $(\lambda = 1, \mu = 0)$, which we know will be present for all higher order normal forms. The degeneracy at $(\lambda = -1, \mu = 0)$ of the first nontrivial normal form is solved however by the second nontrivial normal form. Another Hamiltonian Hopf bifurcation has now appeared at $(\lambda = X, \mu = 0)$.

We have also seen that the usage of different sets of coordinates can simplify equations a lot (but the cost is that they are harder to interpret), making some algebraic tricks possible. In the case of the centre-saddle bifurcation we had to switch to the usage of the nodal-Lissajous variables in order to obtain an analytical expression of the bifurcation line.

In the new region that emerged in the parameter plane between the centre-saddle bifurcation line and the flip bifurcation line global bifurcations occur. We have shown that this happens, no matter what the value of $\delta > 0$ is, at $(\lambda = -1, \mu = 0)$. The global bifurcation line divides region 2 into two new sections, and we have seen that the global bifurcation line touches the line of centre-saddle bifurcations once in the plane $\mu > 0$.

References

- [1] Cotter, C. (1986). *The 1:1 semi-simple resonance*, Ph.D. Thesis, University of California at Santa Cruz.
- [2] Cushman, R., Ferrer, S., Hanßmann, H. (1999). Singular reduction of axially symmetric perturbations of the isotropic harmonic oscillator. *Nonlinearity* **12**, 389-410.
- [3] David, D., Holm, D., Tratnik, M. (1990). Hamiltonian Chaos in Nonlinear Optical Polarization Dynamics. *Physics Reports* **187**, 281-367.
- [4] Ferrer, S., Hanßmann, H., Palacián, J., Yanguas, P. (2002). On perturbed oscillators in 1:1:1 resonance: The case of axially symmetric cubic potentials. *J. Geom. Phys.* **40**, 320-369.
- [5] Ferrer, S., Lara, M., Palacián, J., San Juan, J.F., Viartola, A., Yanguas, P. (1998). The Hénon and Heiles problem in three dimensions. II. Relative equilibria and bifurcations in the reduced system. *Int. J. Bifurc. Chaos Appl. Sci. Eng.* **8**, 1215-1229.
- [6] Gelfand, I., Kapranov, M., Zelevinsky, A. (1994). *Discriminants, resultants, and multidimensional determinants*, Birkhäuser.
- [7] Hanßmann, H., Van der Meer, J. C. (2002). On the Hamiltonian Hopf bifurcations in the 3D Hénon-Heiles family. *J. Dyn. Diff. Eq.* **14**, 675-695.
- [8] Hanßmann, H., Van der Meer, J.C. (2005). Algebraic Methods for Determining Hamiltonian Hopf Bifurcations in Three-Degree-of-Freedom Systems. *J. Dyn. Diff. Eq.* **17**, 453-474.
- [9] Hanßmann, H., Sommer, B. (2001). A degenerate bifurcation in the Hénon-Heiles family. *Celes. Mech. Dyn. Astron.* **81**, 249-261.
- [10] Miller, B.R. (1991). The Lissajous transformation - III. Parametric bifurcations. *Celes. Mech. Dyn. Astron.* **51**, 251-270.
- [11] Yanguas, P. (1998). *Integrability, normalization and symmetries of Hamiltonian systems in 1-1-1 resonance*, Ph.D. Thesis, Universidad Pública de Navarra.

- [12] De Zeeuw, T., Merrit, D. (1983). Stellar orbits in a triaxial galaxy. I. Orbits in the plane of rotation. *Astrophys. J.* **267**, 571-595.